Multi-objective property optimisation of a phosphoserine-modified calcium phosphate cement for orthopaedic and dental applications using design of experiments methodology

Tzagiollari, A., Redmond, J., McCarthy, H. O., Levingstone, T. J., & Dunne, N. J. (2024). Multi-objective property optimisation of a phosphoserine-modified calcium phosphate cement for orthopaedic and dental applications using design of experiments methodology. *Acta Biomaterialia*, *174*, 447-462. https://doi.org/10.1016/j.actbio.2023.11.024

Published in:
Acta Biomaterialia

Document Version:
Publisher's PDF, also known as Version of record

Acta Biomaterialia 174 (2024) 447–462

Contents lists available at ScienceDirect

Acta Biomaterialia

journal homepage: www.elsevier.com/locate/actbio

Full length article

Multi-objective property optimisation of a phosphoserine-modified calcium phosphate cement for orthopaedic and dental applications using design of experiments methodology

Antzela Tzagiollari[a,b], John Redmond[a,b], Helen O. McCarthy[c], Tanya J. Levingstone[a,b,d,f,g,i,j], Nicholas J. Dunne[a,b,c,d,e,g,h,i,j,*]

[a] *School of Mechanical and Manufacturing Engineering, Dublin City University, Dublin 9, Ireland*
[b] *Centre for Medical Engineering Research, Dublin City University, Dublin 9, Ireland*
[c] *School of Pharmacy, Queen's University Belfast, Belfast BT9 7BL, United Kingdom*
[d] *Biodesign Europe, Dublin City University, Dublin 9, Ireland*
[e] *Department of Mechanical and Manufacturing Engineering, School of Engineering, Trinity College Dublin, Dublin 2, Ireland*
[f] *Tissue, Engineering Research Group, Department of Anatomy and Regenerative Medicine, Royal College of Surgeons in Ireland, Dublin 2, Ireland*
[g] *Advanced Manufacturing Research Centre (I-Form), School of Mechanical and Manufacturing Engineering, Dublin City University, Dublin 9, Ireland*
[h] *Advanced Materials and Bioengineering Research Centre (AMBER), Trinity College Dublin, Dublin 2, Ireland*
[i] *Trinity Centre for Biomedical Engineering, Trinity Biomedical Sciences Institute, Trinity College Dublin, Dublin 2, Ireland*
[j] *Advanced Processing Technology Research Centre, Dublin City University, Dublin 9, Ireland*

A R T I C L E I N F O

Article history:
Received 4 July 2023
Revised 10 November 2023
Accepted 15 November 2023
Available online 23 November 2023

Keywords:
Bioinspired adhesives
Phosphoserine
Bone stabilisation
Amino acids
Fracture repair

A B S T R A C T

Phosphoserine is a ubiquitous molecule found in numerous proteins and, when combined with alpha-tricalcium phosphate (α-TCP) powder, demonstrates the ability to generate an adhesive biomaterial capable of stabilising and repairing bone fractures. Design of Experiments (DoE) approach was able to optimise the composition of phosphoserine-modified calcium phosphate cement (PM-CPC) demonstrating that the liquid:powder ratio (LPR) and quantity of phosphoserine (wt%) significantly influenced the handling, mechanical, and adhesion properties. Subsequently, the DoE optimisation process identified the optimal PM-CPC formulation, exhibiting a compressive strength of 29.2 ± 4.9 MPa and bond/shear strength of 3.6 ± 0.9 MPa after a 24 h setting reaction. Moreover, the optimal PM-CPC composition necessitated a mixing time of 20 s and displayed an initial setting time between 3 and 4 min, thus enabling homogenous mixing and precise delivery within a surgical environment. Notably, the PM-CPC demonstrated a bone-to-bone bond strength of 1.05 ± 0.3 MPa under wet conditions, coupled with a slow degradation rate during the first five days. These findings highlight the ability of PM-CPC to effectively support and stabilise bone fragments during the initial stages of natural bone healing. The developed PM-CPC formulations fulfil the clinical requirements for working and setting times, static mechanical, degradation properties, and injectability, enabling surgeons to stabilise complex bone fractures. This innovative bioinspired adhesive represents a significant advancement in the treatment of challenging bone injuries, offering precise delivery within a surgical environment and the potential to enhance patient outcomes.

Statement of significance

This manuscript presents a noteworthy contribution to the field of bone fracture healing and fixation by introducing a novel phosphoserine-modified calcium phosphate cement (PM-CPC) adhesive by incorporating phosphoserine and alpha-TCP. This study demonstrates the fabrication and extensive characterisation of this adhesive biomaterial that holds great promise for stabilising and repairing complex bone fractures. Design of Experiment (DoE) software was used to investigate the correlations between process, property, and structure of the adhesive, resulting in a cost-effective formulation with desirable

* Corresponding author at: School of Mechanical and Manufacturing Engineering, Dublin City University, Dublin 9, Ireland.
E-mail address: nicholas.dunne@dcu.ie (N.J. Dunne).

https://doi.org/10.1016/j.actbio.2023.11.024

physical and handling properties. The PM-CPC adhesive exhibited excellent adhesion and cohesion properties in wet-field conditions. This research offers significant potential for clinical translation and contributes to the ongoing advancements in bone tissue engineering.

1. Introduction

Complex bone fractures present significant challenges in healthcare, often requiring complex surgical intervention and leading to poor clinical outcomes. The Global Burden of Diseases report in 2019 highlighted a substantial increase of approximately 70 % in new bone fracture cases since 1990, with 145 million new cases reported [1]. While the natural healing process of bone fracture is generally effective [2,3], the use of metal hardware is a common approach in the treatment of post-traumatic injuries. However, metal hardware [4] has limitations and often results in poor healing and a lack of mechanical integrity, particularly in fractures occurring in patients with osteoporosis [5]. Bone plates, screws and pins tend to loosen over time, necessitating their removal, which can lead to cortical bone loss [6,7]. Additionally, there is currently no convenient method to stabilise small bone fragments and prevent micromotion in cases involving multiple bone fragments resulting from multiple breaks.

To address these challenges, several biological-based adhesives have been developed to minimise the need for metal hardware and subsequent revision surgeries, thereby improving surgical efficiency, cost-effectiveness, and patient safety [8–10]. Calcium phosphate cements (CPC) have gained significant attention for bone replacement applications due to their moldability, osteoconductivity, and biodegradability. CPC are formed by mixing a solid calcium phosphate powder with a liquid phase, resulting in mineral crystallisation and cement hardening [11]. CPC are classified into acidic cements (monetite or brushite) and basic cements (apatite or calcium-deficient hydroxyapatite) both of which have surface chemistry similar to the mineral phase of bone, making them suitable as bone void fillers [12]. However, CPC still exhibit inferior physical and biological properties compared to native tissue due to their brittle nature and poor tensile and shear properties resulting from randomly organised networks of entangled crystals [13,14]. The lack of effective commercially available bone adhesives can be attributed to the complex criteria for adequate bone repair, which include mechanical stability in wet conditions, sufficient working time for the surgeon, osteogenesis, and biocompatibility [8].

In an effort to improve the mechanical characteristics and overall efficacy of CPC, an array of inorganic fibres and fillers, including materials like bovine collagen, poly(lactic acid) (PLA), poly(glycolic acid) (PGA), poly(lactic-co-glycolic acid) (PLGA), and others, have been extensively used for physicochemical enhancements. This strategic approach has yielded notable improvements in bone fracture healing, rendering it more effective and expeditious [15–19]. Nonetheless, the practical utility of these materials in clinical contexts remains constrained due to persistent challenges, such as poor injectability [20,21], limited elasticity [22] and suboptimal degradability [23–26]. Studies have also focused on incorporating synthetic monomers/polymers to improve mechanical properties, achieving higher compressive, bend, and bond strength, as well as fracture toughness [27–31]. However, this comes at the expense of dissolution and resorption rates [32,33].

Amino acids offer a promising alternative to synthetic monomers, organic acids, or chemical modification. Specifically, amino acid additives can enhance handling and setting properties of CPC, template mineralisation of nanoscale amorphous calcium phosphate, stabilise metastable ceramic phases, improve mechanical properties, promote cell attachment, survival, and proliferation [34,35]. Amino acids can introduce macroscale disorder in cements by adsorbing to crystal surfaces or incorporating into the crystal lattice, potentially increasing the dissolution rate and the release of bioactive ions such as calcium and phosphate [36–39]. Phosphoserine, an amino acid predominantly found in phosphoproteins like osteopontin (OPN), plays a crucial role in various biological processes. OPN, a non-collagenous bone sialoprotein, is involved in mineralisation in vertebrates and contributes to multiple functions such as adhesion/cohesion of both hard and soft tissue under wet-field environments, load dissipation in animals, and the biomineralisation of calcium phosphate precipitation through matrix proteins and matrix vesicles [40,41]. When synthetic amorphous calcium phosphates, such as α-TCP, are exposed to biological fluids, they undergo transformation into metastable phases such as octacalcium phosphate (OCP) or directly convert into hydroxyapatite (HA) within a relatively short period. This transformation leads to a rapid resorption and mineralisation of cells onto the cement surface, facilitating the release of bioactive ions [42–44].

Phosphoserine has been demonstrated to hold a prominent role in augmenting the handling and mechanical attributes of α-TCP cements, while also promoting cellular proliferation and differentiation [41,45]. The integration of phosphoserine as an adjuvant in α-TCP-based cements facilitates the replication of complex architectural and material features, culminating in enhanced properties, relating to stability under hydrated conditions [46–51] and adhesive capabilities, particularly pertinent in the context of dental implant applications [52]. Remarkably, these modified cements exhibit wet-strength values of 40–100 times higher than those of commercial cyanoacrylates and surgical fibrin glues, while establishing a nanoscale organic/inorganic microstructure and facilitating templating of nanoscale amorphous calcium phosphate nucleation [23,47]. Furthermore, adhesive formulations modified with phosphoserine exhibited high adhesion strength without eliciting any adverse effects to adjacent tissues. The introduction of phosphoserine to CPCs expedited the setting reaction [53,54], and encouraged cellular proliferation and differentiation [41]. While this body of research underscores the considerable promise of phosphoserine-modified adhesives in tissue repair, there remains a notable gap in comprehending the influence of various process parameters on the adhesive's properties [55–59]. Additionally, it is imperative to systematically tailor the adhesive composition to align with the distinct clinical requirements of diverse application sites and fracture patterns. Thus, it is necessary to identify a composition that can effectively tailor the relevant properties to achieve efficacy and effectiveness.

In addition to organic acids, the presence of inorganic silicic acid salts, such as calcium silicate, can exert significant influence on the characteristics of adhesive-based biomaterials. Calcium silicate is well-recognised for its osteoconductive properties and its ability to promote the formation of hydroxyapatite [60]. For example, the incorporation of calcium silicate into magnesium phosphate cements has been documented to not only enhance mechanical properties but also to exhibit *in vitro* apatite mineralisation, bioactivity, and biodegradation capabilities [61,62]. This interaction with the body's natural processes promotes integration between the adhesive material and the surrounding bone tissue, thereby augmenting bonding strength and overall stability [63,64]. Moreover, *in vivo* investigations have demonstrated that biomaterials containing calcium silicate can stimulate osteogenesis by accelerating new bone formation [65]. Furthermore, it is essential to note that calcium silicate's physicochemical properties can impact crucial parameters, including setting time, viscosity, and workability of the adhesive material. Consequently, these properties can influence the ease of surgical application and the subsequent clinical performance of the adhesive material [66].

Developing an optimised formulation of bone adhesive that meets clinical requirements in a short period is a crucial challenge. Thus, computer-based optimisation techniques, such as a Design of Experiments (DoE) approaches based on response surface methodology (RSM), are frequently employed to speed up the process and avoid bottlenecks. This method employs appropriate experimental designs and polynomial equations to determine the optimal operating conditions for a given system or the specific modifications induced by a set of variables within defined regions of interest. In this study, we used the DoE methodology to investigate the correlations between process, property, and structure of phosphoserine-modified calcium phosphate cement (PM-CPC), including α-TCP (as the main calcium phosphate), phosphoserine, and calcium silicate. The aim of this study was to facilitate the development of an ideal PM-CPC composition with desirable physical and handling properties that enable it to be effectively applied by surgeons to stabilise challenging fractures and dental implants, and achieve rapid and sufficient stabilisation. Furthermore, this composition must provide sufficient adhesion and cohesion properties under wet-field conditions while minimising experimentation resources and time, thereby establishing a cost-effective formulation compared to conventional methods.

2. Materials and methods

2.1. DoE analysis & optimisation study

A DoE-based study was used to investigate the relationships between multiple input and output variables in the context of the PM-CPC synthesis. To accommodate the complexity of factors involved, a Box–Behnken three-level factorial design was implemented, using Design-Expert V5 Software (Stat-Ease Inc., USA). DoE methods have emerged a cost-effective means for determining the individual influence of variables and their interactions, surpassing the limitations of traditional 'one-at-a-time experimental' methods. The experimental design consisted of five factors: four numerical factors A (liquid:powder ratio [LPR], B: (weight% [wt%] phosphoserine), C (wt% Ca_2SiO_4), and D (number of grinding cycles); and one categorical factor denoted as E: (post-process) (Table 1). Notably, it was observed from the initial results that particle size demonstrated a significant impact on the properties of PM-CPC. Consequently, three distinct studies were conducted, each exploring a specific range of grinding cycles while maintaining consistent levels for the remaining factors. These studies were identified as Study 1 where the particles underwent 2, 6 and 10 grinding cycles, Study 2 exploring 9, 11 and 13 grinding cycles, and Study 3 which investigated 13, 15 and 17 grinding cycles.

Upon completion of the experimental testing phase, the collected data were analysed using the DoE software. Regression equations were derived to ascertain the significance of the terms within each equation, employing sequential F-tests, lack-of–fit evaluations, and the Analysis of Variance (ANOVA) method. Statistical significance was considered to be a p-value below 0.05. The Whitcomb Score, a recognised metric in the field [67], was used to select the most suitable model(s) and determined the influence of every factor on every response. To determine the optimal composition of PM-CPC, numerical optimisation approach was used, guided by the following criteria: initial setting time (t_i) $\geq$ 60 s, final setting time (t_f) $\leq$ 200 s, compression strength $\geq$10 MPa [68], and bond strength $\geq$ 2.5 MPa [69]. Inputs from the orthopaedic surgical community were sought to establish clinically relevant setting times (t_i and t_f) that would facilitate rapid setting, achieve the required fragment stability and prevent adhesive leakage [70]. These setting times were considered as the most important responses in the optimisation process. The DoE optimisation was conducted using the desirability function approach, where each response was assigned a desirability function (d_i). The d_i value ranged between 0 and 1, with 0 representing that the worst acceptable value and 1 denoting the optimal performance with respect to the studied factors. Subsequently, the optimal composition of PM-CPC was identified, followed by synthesis and evaluation to validate the DoE study.

2.2. Fabrication of α-TCP powder

The first step in the process involved the synthesis and characterisation of α-TCP for use in PM-CPC fabrication. The α-TCP powder was obtained by thermal transformation of a mixture of calcium phosphate ($CaHPO_4$) and calcium carbonate ($CaCO_3$) (Sigma Aldrich, Ireland) at a molar ratio of $Ca/P \approx 3{:}2$, using a temperature of 1400 °C for 360 min [71]. In some cases, a post process passivation step was performed to reduce any remaining defects or impurities by reheating the powder to 500 °C for 24 h.

To prepare the α-TCP powder for the DoE study, it was mixed with ethanol and subjected to grinding using a planetary mill (Pulverisette 6, Frisch, Germany) with 50 agate balls of 10 mm diameter. The mill was operated at a rotating speed of 600 ± 5 RPM for a specified number of cycles ranging from 2 to 17 cycles, as determined by study design. Each grinding cycle consisted of 5 min of grinding followed by a 5-min dwell time between each grinding cycle.

2.3. PM-CPC fabrication

Various formulations of PM-CPC were synthesized by blending the liquid phase (Deionized (DI) water) with the pre-mixed powder phase at concentrations specified by the DoE framework (Table 1). The powder phase was composed of α-TCP, phospho-

Table 1
Numerical and categorical factors and their corresponding levels used for the three different DoE studies that explored the effect of varying grinding cycles.

Factors	Units	Levels	Responses
Numerical: LPR	mL/g	0.2; 0.35; 0.5	t_i (s)
Numerical: Phosphoserine	wt%	10; 25; 40	t_f (s)
Numerical: Ca_2SiO_4	wt%	0; 1; 2	Compressive Strength (MPa)
Numerical: Grinding Cycles	–	Study 1: 2; 6; 10 Study 2: 9; 11; 13 Study 3: 13; 15; 17	Bond Strength (MPa)
Categorical: Post-process	–	Passivation Non-Passivation	

serine (Flamma, S.p.A. Italy), and calcium silicate (Sigma Aldrich), each with predefined weight percentages (wt%), ranging from 10 % to 40 % for phosphoserine and 0 % to 2 % for calcium silicate. DI water was added at a predetermined LPR ranging from 0.2 mL/g to 0.5 mL/g. In each experimental run as defined by the DoE study, a total of 1 g of PM-CPC underwent manual mixing until all constituent elements were thoroughly blended, ensuring uniformity and consistency throughout. The determination of mixing completion was based on visual examination, with the mixture assessed for uniformity and consistency. The achievement of complete homogeneity was denoted by a noticeable transformation in the adhesive's texture, rendering it smooth and glossy. Subsequently, the homogeneous blend was placed into PTFE moulds, thereby yielding samples with the required shapes and dimensions necessary for subsequent characterisation methodologies. All samples were set for 72 h in Ringer's solution at 37 °C and 100 % relative humidity to simulate the biological environment.

2.4. Analytical assessment – α-TCP powder

2.4.1. Chemical properties

Qualitative validation of the α-TCP powder was performed through X-Ray Diffraction (XRD) analysis using a Bruker D8 diffractometer (Bruker, Germany). Scans were conducted with a scan speed of 2 s/scan at 30 kV and 10 mA, using Cu-Kα radiation in the 2θ range of 20–60°. The peaks in the spectra were identified using Rietveld analysis (Profex software) and compared to the International Centre for Diffraction Data (ICDD) diffraction patterns for α-TCP (ICDD923), hydroxyapatite (HA) (ICDD432), beta-tricalcium phosphate (beta-TCP) (ICDD619) and beta-calcium pyrophosphate (beta-CPP) (ICDD169).

2.4.2. Physical properties

The particle size distribution was determined using a Malvern Mastersizer Particle Analyser (Malvern Panalytical, UK) in accordance with ISO 13320 [72]. The values of D_{10}, D_{50} and D_{90} were recorded, representing the cumulative distribution at 10 %, 50 % and 90 % of the total distribution of particle sizes. The results were reported in µm with six replicates per sample.

Surface analysis was conducted using Laser Diffraction (LD) analysis (Malvern Zetasizer Ultra) to measure the zeta potential of the α-TCP suspended in DI water with a refractive index of 1.58.

Scanning Electron Microscopy (SEM) analysis of the powder particles was performed using the Zeiss EVOLS15 Scanning Electron Microscope (ZEISS, Germany) at an acceleration voltage of 15 kV extra-high tension (EHT). Prior to imaging, the powder samples were sputter-coated with gold to enhance conductivity. The morphology of the powders was assessed using Image J software (version 1.8.0_172, NIH, USA).

2.5. Analytical assessment – doe study

2.5.1. Setting properties

The t_i and t_f setting times of the PM-CPC compositions were determined using the Gilmore needle apparatus [73], in accordance with ASTM C266-99. The experimental setup comprised two weighted needles, one weighing 113.4 ± 0.5 g, and another weighing 453.6 ± 0.5 g for measuring the t_i and t_f, respectively. The 't_i' value signifies the time when adhesive solidification initiates upon application, permitting its use at the surgical site while maintaining its workability for effective delivery. Conversely, the 't_f' value marks the point at which the adhesive attains its peak strength and stability, establishing a complete bond between tissues that hinders subsequent adjustments due to the potential risk of disrupting the bond. In each iteration of the DoE study, a total of 1 g of PM-CPC (containing the appropriate proportions of α-TCP, phosphoserine, and calcium silicate) was solubilised in DI water and subsequently manually blended. The homogenous mixture of PM-CPC was transferred into custom-made polytetrafluoroethylene (PTFE, Radionics, RS Stock No.:680-678) moulds (h = 8 mm, d = 10 mm). The adhesive was injected into each mould using a conventional 5 mL syringe which had an extrusion diameter of 2.25 mm. The test was conducted in Ringer's solution at 37 °C to simulate the biological environment.

2.5.2. Mechanical properties

To assess the static mechanical properties of the various PM-CPC, compression, compression tests (ISO5833:2002) [74] and bond strength tests were performed. For the compression test, PM-CPC samples was transferred to PTFE moulds (12 mm height, 6 mm diameter). For the bond strength testing, a 0.25 g layer of PM-CPC was applied to one surface of a 100 mm^2 stainless steel cube, and a second stainless steel cube was placed on top of the PM-CPC layer. The two cubes were clamped together using universal grips. Samples were then incubated in Ringer's solution at 37 °C for 72 h before testing. A Zwick Testing Machine (Zwick Roell, UK) equipped with a 5 kN load cell was used for both compression and adhesion testing, with a crosshead speed of 1 mm/min. The samples were tested until failure, and the compressive strength and bond strength were determined from the resultant stress–strain curves.

2.6. Analytical assessment – optimal PM-CPC

2.6.1. Setting and mechanical properties

To assess the clinical applicability of the adhesive, additional characterisation of the optimal PM-CPC was conducted. The scalability of the optimal PM-CPC was evaluated by increasing the batch size from 1 g to 10 g. The setting characteristics of the optimised PM-CPC adhesive for varying batch sizes were assessed using the Gilmore needle test, in accordance with Section 2.5.1. Visual evaluation was conducted during the injection process into each PTFE mould to assess the injectability and ease of handling of the PM-CPC. The PTFE moulds were immersed in a temperature-controlled water bath held at 37 °C for the duration of the testing. Following injection, the workability of the PM-CPC was evaluated by manipulating it with a spatula. The time that the PM-CPC adhesive maintained its injectability and workability were recorded. Furthermore, the mechanical properties of the optimal PM-CPC adhesive from each batch size were determined in line with the protocols outlined in Section 2.5.2.

2.6.2. Washout resistance

The stability of the PM-CPC in a wet-field environment simulating the biological environment was assessed using a washout resistance test [75]. The optimal PM-CPC was manually shaped into a ball (volume ≈ 0.50 mm^3) and placed in a 6-well plate containing 10 mL of phosphate buffer solution (PBS). The sample was incubated at 37 °C and visually inspected every minute for 5 min. The sample was considered to have passed the disintegration test if it did not visibly disintegrate in the solution.

2.6.3. Degradation properties

Cylindrical PM-CPC samples (12 mm height, 6 mm diameter) were incubated in PBS solution (pH 7.4) at 37 °C on a plate shaker for time intervals of 4, 6, 8, 14, 30, 60, 90, and 120 days. The solution was replaced every 4 weeks. At each time-point, three samples were removed from the degradation media, washed with DI water, and dried under vacuum for 2 days at 37 °C. The dry mass of the samples was then determined.

For the enzymatic-based *in vitro* degradation, a porcine pancreas lipase (PPL)-PBS was used instead of PBS. The PPL concentration was 10 U/mL PPL (≥3000 U/g, Merck Life Science Limited, Ireland). The procedure as with PBS was followed.

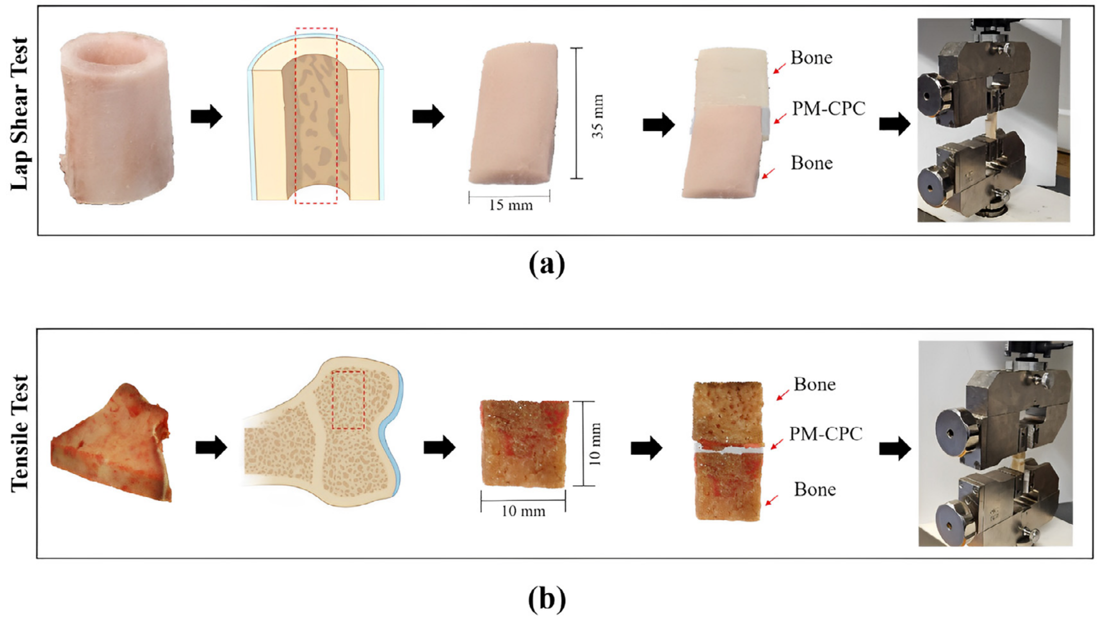

Fig. 1. Schematic overview representing the arrangements employed for the mechanical assessment of porcine bovine femur bone samples, encompassing both cortical and cancellous bone sections, joined through the application of PM-CPC adhesive. Specifically, arrangements for a) lap shear and b) tensile testing, as performed within the Zwick testing apparatus.

2.6.4. Bioactivity

To evaluate the bioactivity, the formation of bone-–like apatite on the samples (4 mm height, 8 mm diameter) was examined in a simulate body fluid solution, at 37 °C and pH of 7.4. The ion concentrations in the solution was almost identical to those in human blood plasma [76]. The solution was replenished every 3 days while the samples were removed after 24 h, 3 days and 7 days. Subsequently, the samples were washed with DI water and dried in an oven at 50 °C for 3 h. Changes in the surface morphology of samples were characterised using SEM (Section 2.4.1) equipped with energy-dispersive X-ray spectroscopy (EDX) (Section 2.4.1).

Additionally, XRD analysis (Section 2.4.1) was performed to evaluate the crystalline phases present in the PM-CPC at different time points, including after mixing and during the setting reactions. The XRD analysis was performed after 24 h, 3 days, and 7 days to assess the time-dependent phase transition. For this analysis, each sample was dried and ground to a powder using a mortar and pestle.

2.7. Bone to bone adhesion properties – optimal PM-CPC

a) Sample Preparation

Bovine femora were purchased to obtain samples of both cortical and cancellous bone The bones were sectioned into rectangular slices measuring 35 × 15 × 3 mm ($n = 6$)) and cuboid-shaped samples measuring 20 × 20 × 10 mm ($n = 6$)) using a Titan TTB705BDS electric bandsaw (Screwfix, Ireland) with water cooling. To ensure uniform thickness, the bone samples were ground using a Metkon Forcimat (Bursa, Turkey) grinding–polishing machine with P80-grade silicon carbide paper (TMQ Ltd., Ireland).

a) Characterisation techniques

Lap shear and tensile tests were conducted to assess bone-to-bone adhesion ($n = 6$ samples per test) under dry and wet conditions. The lap shear test used rectangular-shaped bone samples (25 × 10 × 3 mm), while the tensile test employed cuboid-shaped bone samples (10 × 10 × 10 mm). Each test sample was prepared by applying a 0.2 g layer of the optimal PM-CPC to one surface of a bone sample, covering a surface area of 100 mm^2. Subsequently, a second bone sample was positioned on top of the initial bone sample, and both bone samples were securely affixed together using universal grips. Following this, the assembled arrangement was submerged in Ringer's solution and subjected to an incubation period of 72 h at 37 °C. Thereafter, each assembled arrangement was securely clamped within the Zwick Testing System, as illustrated in Fig. 1a and b, and underwent the appropriate mechanical testing until failure, in accordance with the procedures detailed in Section 2.5.2. Fracture surface after failure was examined using SEM-EDX analysis to identify the mode of failure, which could be adhesive (failure between adhesive and bone substrate), cohesive (failure within the adhesive), or mixed (involving both cohesive and adhesive failure).

2.8. Statistical analysis

Statistical analysis of the data generated within the DoE study was completed using the DoE software as described in Section 2.1. A polynomial equation (Eq. 1) was used to model the response variable (Y) as a function of the input factors (X_i, X_j...) as follows:

$$Y = b_0 + \sum_{i=1}^{p} b_i X_i + \sum_{i=1}^{p} \sum_{j=1}^{p} b_{ij} X_i X_j + \sum_{i=1}^{p} b_{ii} X_i^2 \quad i \neq j \tag{1}$$

The coefficients of the polynomial equation were denoted by b_0 (overall mean response), b_i (main effects for each factor), b_{ij} (two-way interaction between the ith and jth factors), as well as b_{ii} (quadratic effect for the ith factor). A comprehensive analysis was conducted, through statistical assessment of the regression model, visualisation of response surface graphs, and determination of optimal process parameter values. Analysis of Variance (ANOVA) was used to determine the significance of the quadratic models, where a p-value < 0.05 was considered as statistically significant. For the "optimal" design, the design points were selected by a statistical criterion such as minimising the uncertainty on the estimated effects.

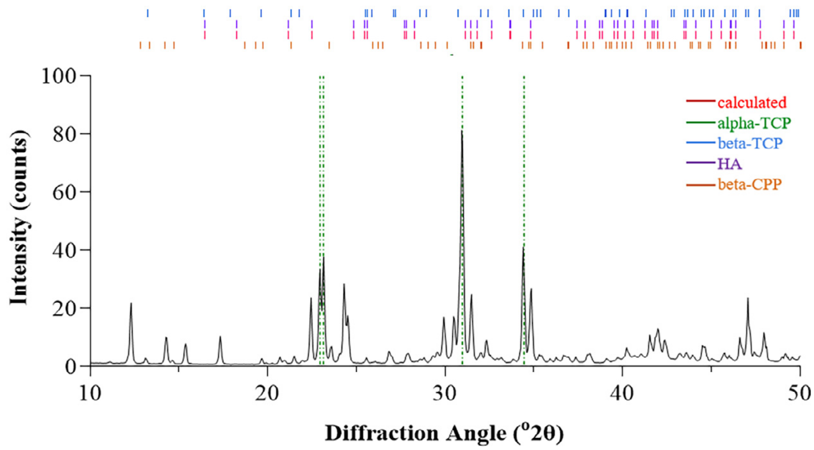

Fig. 2. X-ray diffraction (XRD) pattern confirming the phase composition of the α-TCP powder. Rietveld analysis showed that the XRD pattern matched the reference pattern for α-TCP (ICDD923) with pronounced peaks observed at 2θ angles of 31.8°, 34.0°, and 36.2°. This confirmed the presence of a highly pure α-TCP phase, with a purity of 100 %.

All experiments were completed using a minimum of three repeats ($n = 3$). Data is presented as the mean±SD. The statistical significance of data for validation of DoE accuracy and percentage of difference comparison was determined using t-tests with $p < 0.05$ as the minimal level of significance.

3. Results

3.1. Analytical assessment – α-TCP powder

3.1.1. Physicochemical properties

XRD analysis was performed on the synthesised powders to determine their phase composition. The XRD spectra revealed prominent peaks at 22.74°, 22.93°, 30.70°, 34.16° 2θ positions corresponding to the (211), (112), and (202) crystallographic planes of α-TCP, confirming the presence of α-TCP (Fig. 2). Rietveld analysis confirmed that no additional phases were detected, indicating complete transformation of the $CaHPO_4$ and $CaCO_3$ into α-TCP, resulting in 100 % phase purity without residual calcium phosphates.

Increasing the number of grinding cycles resulted in a reduction in particle size (Table 2), as evidenced by the shift towards smaller particle sizes in both the SEM images and the particle size analysis data (Fig. 3). The particles exhibited a wide range of sizes, with the mean size decreasing with increasing grinding time. The number of grinding cycles had a significant effect on the particle size of the α-TCP powders (p-value < 0.001), with an inverse relationship between grinding cycles and particle size (Fig. 3). The median particle size (D_{50}) decreased from 23.9 ± 0.7 µm for 2 cycles to 4.05 ± 1.3 µm for 17 cycles. Furthermore, increasing the number of grinding cycles also led to a reduction in the quantitative distribution width (D_{span}) compared to samples with a lower numbers of grinding cycles (Table 2). Specifically, D_{span} values of 1.77, 2.50, 2.89 were calculated after 2, 10, and 17 cycles, respectively. The particles displayed an irregular, non-spherical, and polyhedral shape for all the different grinding cycles without any significant differences in circularity among the different particle sizes, with an average circularity across all groups of 0.35 ± 0.2. The particle size distribution exhibited a normal distribution for all batches, with consistent zeta potential values ranging from - 13 mV and −18 mV. Furthermore, the physical characterisation for the α-TCP powder before and after passivation showed the no significant differences (p-value = 0.1) in particle charge, size distribution and morphology.

3.2. Analytical assessment – DOE study

3.2.1. Setting properties

Notably, the range of setting properties decreased significantly with higher grinding cycles, as observed when comparing the data. In the first set of experiments (1st study), grinding cycles of 2, 6, and 10 were used, resulting in an initial setting time (t_i) ranging from 3 to 10 min and a final setting time (t_f) between 4 and 12 min. The second study involved grinding cycles of 9, 11, and 13, which yielded a t_i between 1 min and 5 min and a t_f between 3 min and 6 min values closer to clinical requirements. Lastly, the third study resulted in a t_i range of 0.5–1 min and a t_f between 0.7 min and 1 min. The results indicate a notable trend in the impact of α-TCP grinding cycles on the setting time of the PM-CPC composition. As the number of grinding cycles increased, there was a consistent reduction in both the initial and final setting times. This finding suggests that the grinding process has a significant influence on the solidification properties of the composition. The observed decrease in setting time can be due to several mechanisms. For instance, the grinding cycles contribute to a reduction in particle size and an increase in surface area, leading to enhanced reactivity and faster setting kinetics. Additionally, the grinding process

Table 2
Particle size distribution and zeta potential of α-TCP powder as a function of increasing the particle attrition cycles.

Attrition cycles	$D_{(10)}$ (µm)	$D_{(50)}$ (µm)	$D_{(90)}$ (µm)	D_{span}	Zeta potential
2	6.7 ± 0.4	25.3 ± 0.7	58.6 ± 4.9	1.78	−15.9 ± 2
6	3.7 ± 0.5	13.3 ± 2.4	30.5 ± 5.8	1.98	−13.2 ± 1
10	2.5 ± 0.5	11.7 ± 1.5	28.8 ± 3.2	2.07	−14.8 ± 3
11	2.1 ± 0.4	6.9 ± 1.5	21.0 ± 2.8	2.46	−17.1 ± 3
13	1.9 ± 0.3	6.2 ± 1.5	17.2 ± 3	2.61	−16.4 ± 4
15	1.7 ± 0.3	5.1 ± 1.3	15.8 ± 2.5	2.72	−18.4 ± 2
17	0.9 ± 0.2	4.1 ± 1.3	12.6 ± 2.5	2.88	−15.8 ± 3

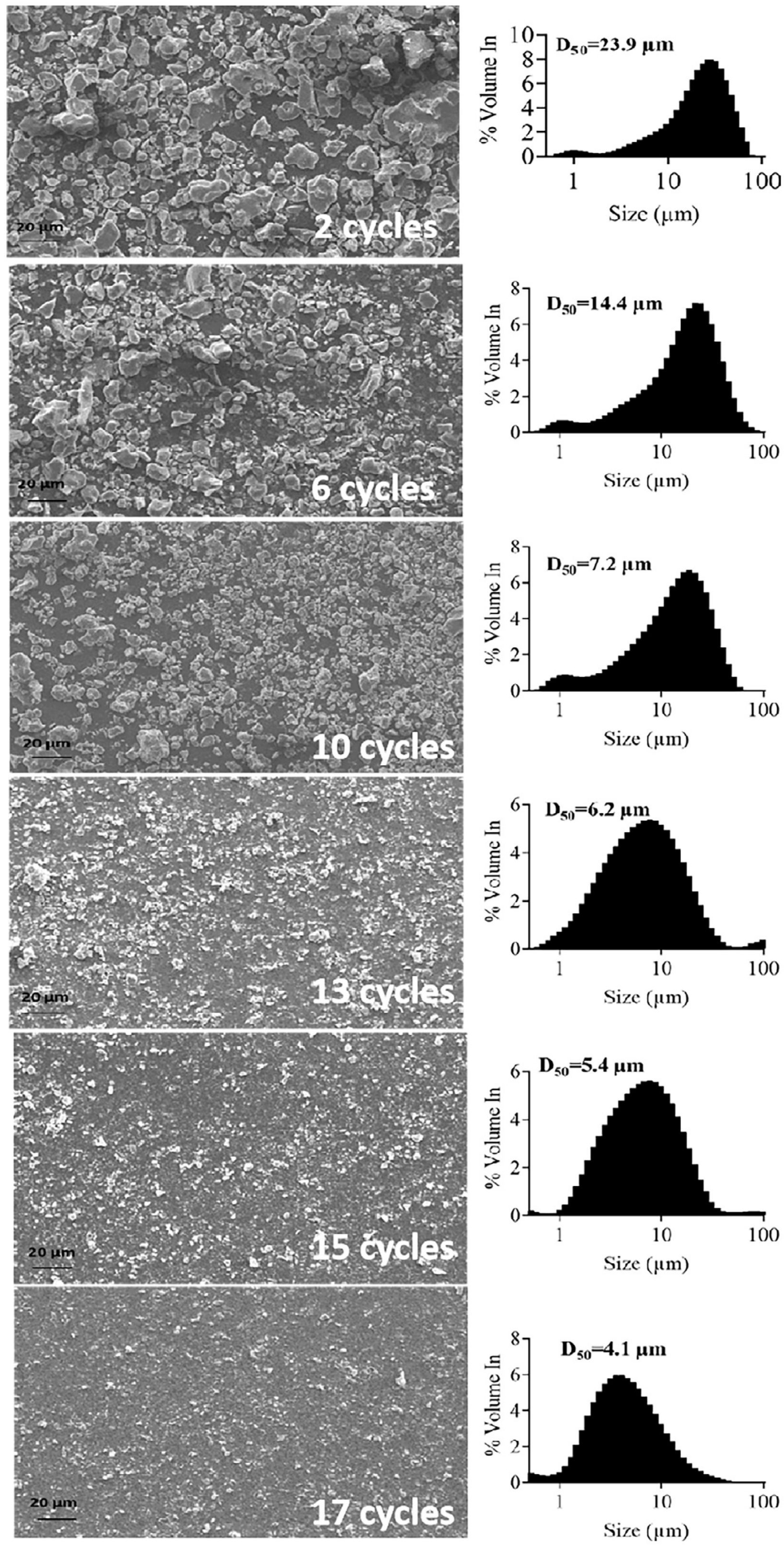

Fig. 3. *SEM and Particle Size Analysis* – SEM images of *α-TCP powder after grinding at different cycles showed* the presence of irregularly shaped particles (non-spherical particles) with a circularity of 0.35 ± 0.2 for all the grinding cycles. *Histograms showing* the particle size distribution of *α-TCP powder after* different grinding cycles. Decrease of particle size was observed increasing the number of cycles from 2 to 17 cycles.

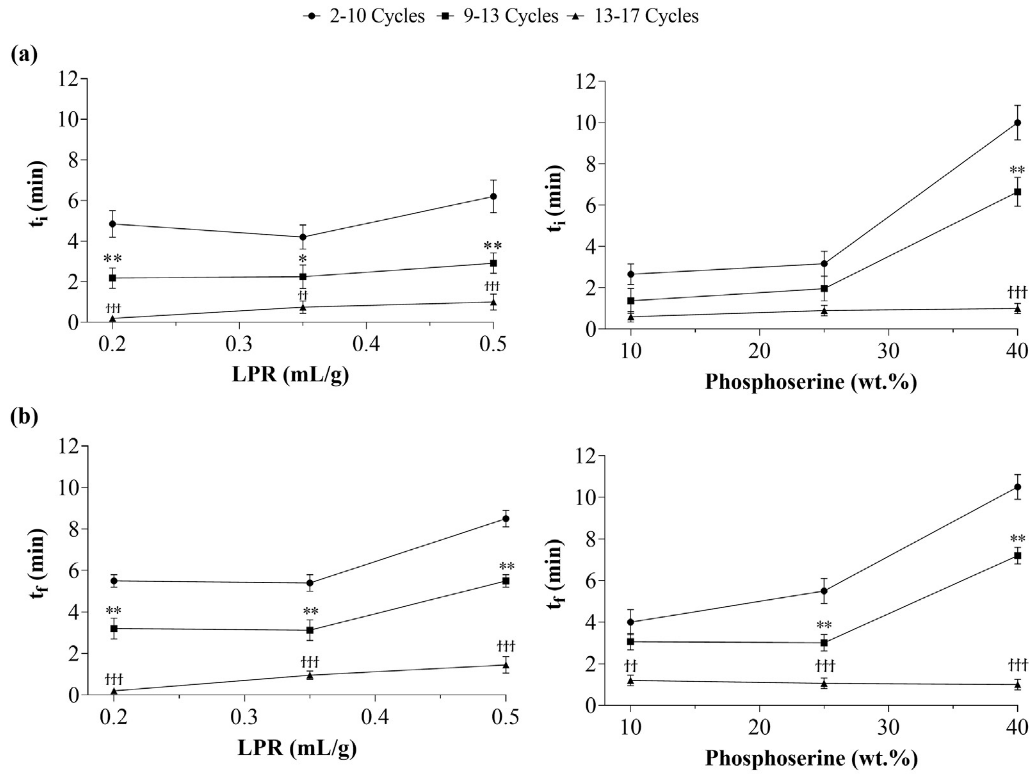

Fig. 4. DoE analytics obtained from Box and Behnken Design studies illustrating the behaviour of the most significant factors. The impact of LPR and phosphoserine content on a) the initial (t_i) and b) the final (t_f) setting time of the PM-CPC adhesive using α-TCP powder at different grinding cycles is shown. The graphs demonstrate that increasing the LPR resulted in slower setting times, while higher amounts of phosphoserine accelerated the setting time. Statistical significance is denoted by $^{*}p$-value < 0.05, $^{**}p$-value < 0.01 at 9–13 cycles and $^{\dagger\dagger}p$-value < 0.01, $^{\dagger\dagger\dagger}p$-value < 0.001 at 13–17 cycles, indicating a decrease in setting time, compared to the values obtained from 2 to 6 cycles.

may introduce defects and microstructural changes, facilitating nucleation and growth of solidification products.

Analysis of the data from all the three different studies using DoE showed that both the t_i and t_f of the PM-CPC had a significant (p-value < 0.001) dependence on the LPR and phosphoserine content, with an interaction between these two factors observed at low grinding cycles (Fig. 4a and b). ANOVA indicated a total variability of 77.77 % in the data, with a non-significant lack-of-fit, confirming the suitability of the model. The ANOVA results further showed that both the LPR and phosphoserine content contributed more than 40 % to the setting properties (i.e., t_i and t_f), while the other factors accounted for 2–7 % of the contribution. For both 1st and 2nd studies it was observed that when the phosphoserine amount was held constant at 25 wt%, an increase in the amount of DI water led to a 30–40 % increase in both t_i and t_f. Conversely, increasing the phosphoserine content from 25 % to 40 % while maintaining a constant LPR of 0.35 mL/g resulted in a rapid three-fold increase in the setting properties. However, 1st, 2nd, and 3rd DoE studies obtained that both t_i and t_f increased significantly with the addition of DI water and phosphoserine, and no differences were observed when comparing the behaviour of the PM-CPC using passivated and non-passivated α-TCP.

Additionally, the smaller particle sizes facilitated easier mixing of the PM-CPC, leading to a significantly reduced (p-value = 0.004) mixing time of 20 s for α-TCP powder that underwent 10–17 grinding cycles, compared to 90 s for α-TCP powder that underwent 2–9 grinding cycles.

3.2.2. Mechanical properties

The compressive strength values obtained from three different studies varying the range of particle grinding cycles for the α-TCP powder used in the PM-CP composition were analysed. In the first study (after 2, 6, and 10 cycles), the PM-CPC samples exhibited compressive strengths ranging from 10 MPa to 30 MPa. In the second study, increasing the grinding cycles and subsequently decreasing particle size, the PM-CPC samples displayed compressive strengths between 10 MPa and 20 MPa. Lastly, the third study obtained the lowest compressive strengths between 5 Mpa and 15 MPa. These results indicate that the compressive strength of PM-CPC is influenced by various factors, including the number of cycles and the composition of the cement. The presence of phosphoserine modification in the PM-CPC composition may contribute to its mechanical properties. The trend of decreasing compressive strength values observed in the third study suggests a potential loss of structural integrity over time. It is worth noting that the compressive strength values obtained in all three studies fall within a similar range, indicating consistent performance. Comparison among the three different DoE studies with varying numbers of particle grinding cycles demonstrated that higher levels of grinding (13–17 cycles) did not impact compressive strength. However, an interaction between phosphoserine content and grinding cycles was observed at high grinding cycles (13–17 cycles) in Study 3, due to aggregation of powder. The use of passivated α-TCP powder showed no statistically significant difference in compressive strength compared to non-passivated α-TCP.

As per DoE analysis, the compressive strength of the different PM-CPC for all the three studies was influenced by two factors: the LPR and the amount of phosphoserine. The ANOVA analysis showed that the LPR has the most significant impact on the compressive strength, contributing more than 20 % to this response. The effects of these factors on the compressive properties are demonstrated in the range of the low and high levels of both the LPR and phosphoserine content (Fig. 5a). A linear relationship was observed between LPR and compressive strength with an in-

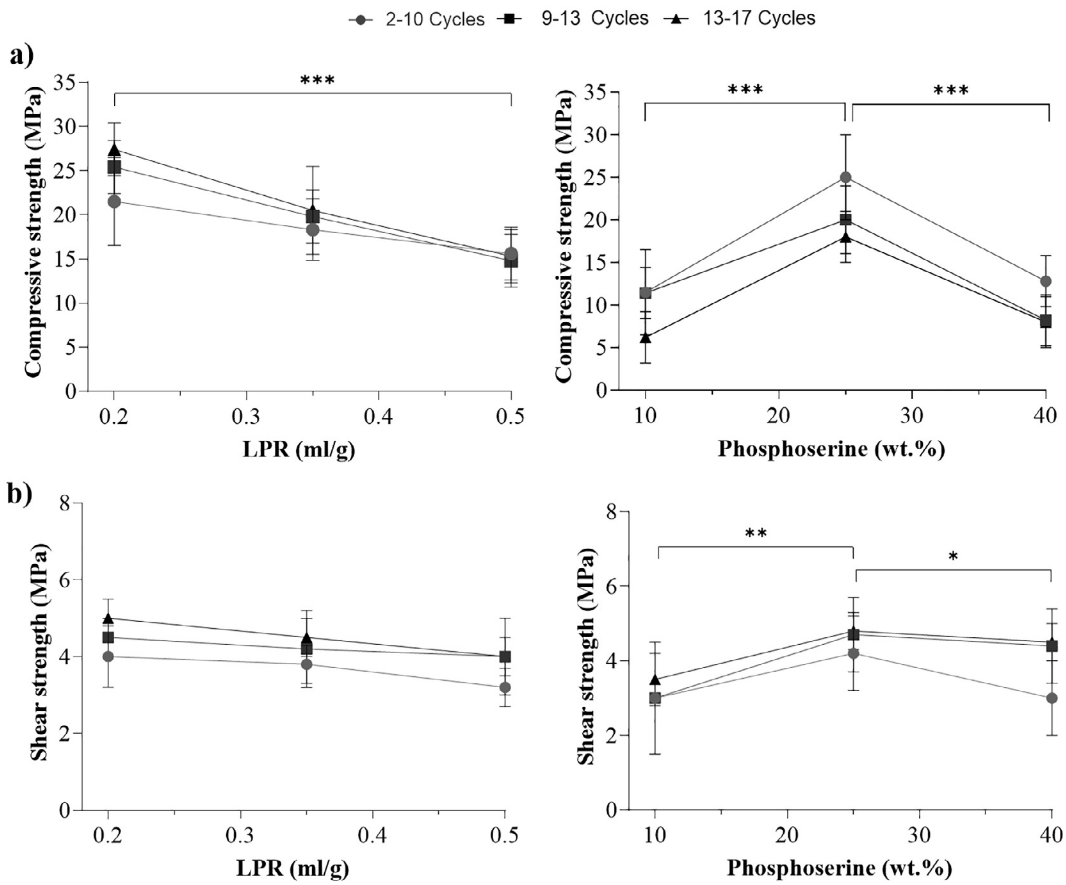

Fig. 5. DoE analytics describing the impact of LPR and phosphoserine content on the mechanical properties of PM-CPC adhesive. The a) Compressive strength and b) bond strength are shown for α-TCP at different grinding cycles. The results demonstrate that increasing the LPR leads to a reduction in compressive strength while not affecting bond strength. Additionally, an increase in phosphoserine content up to 25 % enhanced both compressive strength and bond strength. The significance levels are denoted as *p-value < 0.05, **p-value < 0.01, and ***p-value < 0.001, indicating significant changes observed in all three studies (i.e., 2–6, 9–13, and 13–17 grinding cycles).

crease in the LPR resulting in a reduction in compressive strength. The influence of phosphoserine content on compressive strength displayed a non-linear trend (Fig. 5a). Specifically, increasing the phosphoserine content from 10 to 25 wt% led to an increase in compressive strength up to 25 ± 5 MPa, while higher amounts of phosphoserine caused a decrease in compressive strength in the PM-CPC.

The bond strength of the α-TCP (regardless of the number of grinding cycles) was significantly influenced (p-value < 0.0001) by both the LPR and phosphoserine content (Fig. 5b). The LPR demonstrated a higher contribution of approximately 44 % to the final model, and increasing the LPR led to a decrease in bond strength. Increasing the phosphoserine content enhanced the adhesion properties compared to the addition of DI water, indicating an interrelationship between these two factors. The number of particle grinding cycles did not have a significant impact (p-value $= 0.0501$) on bond strength. However, slightly higher bond strength was observed for α-TCP powder with a smaller particle size (higher number of grinding cycles). An interaction was observed between the number of grinding cycles and the type of α-TCP used (passivated or non-passivated), with higher bond strength observed when using passivated α-TCP prepared using a lower number of particle grinding cycles.

3.2.3. DoE optimisation

The models generated for each response from the DoE analysis were then used to optimise the PM-CPC according to a set of clinical informed optimisation criteria. The optimal PM-CPC composition was determined to be 74 wt% α-TCP (after 11 grinding cycles), 25 wt% phosphoserine, 1 wt% calcium silicate, with a LPR of 0.3 mL/g. This composition achieved a d_i of 0.92, indicating an optimal performance. The predicted responses for the optimal composition of PM-CPC were as follows: an initial setting time ranging from 90 to 110 s, a final setting time ranging from 180 to 240 s, a compressive strength of 25.7 ± 3 MPa and a bond strength of 4.2 ± 0.5 MPa. To verify the accuracy of these predicted values, an experimental validation study was conducted using t-test analysis. The results showed a non-significant difference (p-value $= 0.1$) between the predicted and experimental values, with a percentage of difference lower than 5 % for both setting properties and <14 % for mechanical properties (Table 3). The experimental setting properties for the optimal PM-CPC were as follows: t_i of 115 ± 15 s and a t_f of 192 ± 10 s, and a mixing time of 20 s. The measured compressive strength (24.5. ± 5 MPa) and bond strength (3.9 ± 0.5 MPa) data were also consistent with the predicted values. Furthermore, the DoE studies demonstrated high accuracy, as the experimental values were within the standard deviation (SD) of the predicted responses, with a difference of only 5 % between experimental and predicted values.

3.3. Analytical assessment – optimal PM-CPC

3.3.1. Setting and mechanical properties

While filling each mould for evaluating setting times via the Gilmore needle test, it was visually observed that the injectability of the optimised PM-CPC was maintained for approximately 80 s.

Table 3
Comparison of actual experimental and DoE-predicted data for the optimal PM-CPC composition. T-test analysis reveals no significant difference between the predicted vs actual experimental data for a) initial, b) final setting time, c) compressive and d) bonding strength, confirming the accuracy of the predicted values. All experimental measured values meet the clinical acceptable ranges (initial setting time, t_i = 90–120 s; final setting time, $t_f \leq 240$ s; compression strength ≥10 MPa; bond strength ≥2.5 MPa).

Responses	DoE prediction	Experimental values	Difference (%)
Initial setting time	110 ± 10 s	115 ± 10 s	**4.44**
Final setting time	200 ± 20 s	192 ± 10 s	**4.08**
Compressive strength	25.7 ± 3 MPa	29.5 ± 4.6 MPa	**13.8**
Adhesive strength	4.2 MPa	3.9 ± 0.9 MPa	**7.41**

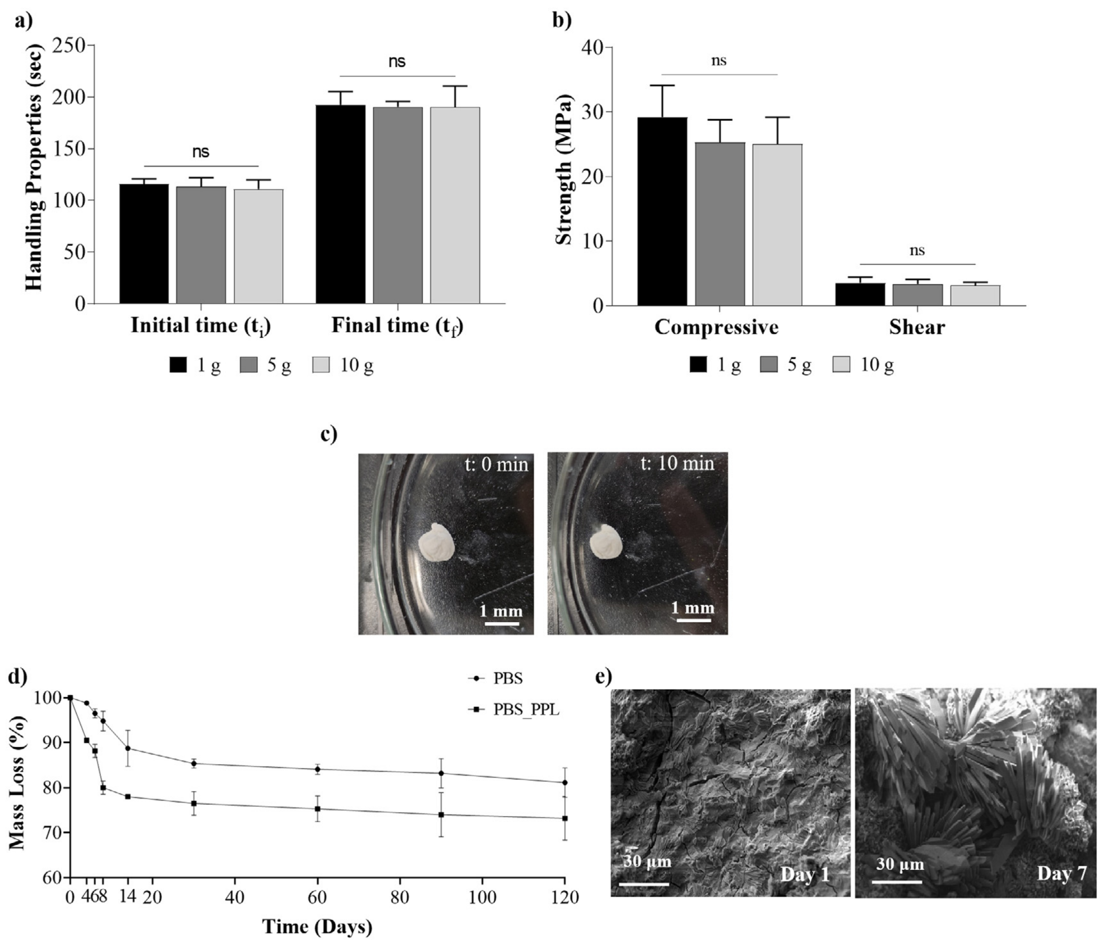

Fig. 6. Characterisation of the optimal PM-CPC adhesive fabricated using a batch size of 1 g, 5 g and 10 g. The a) initial and final setting times and b) mechanical properties were not affected by the batch size. c) Evaluation of the washout resistance showed no disintegration at 10 min after setting. d) Degradation analysis of the PM-CPC immersed in PBS and PBS-PPL at 37 °C, demonstrated a total mass loss of 20 % and 28 % respectively after 120 days, which is consistent with the normal bone healing. e) SEM images showing the extent of bioactivity and conversion of the α-TCP to HA crystals with approximately 50 % of the crystals present showing a needle-shaped morphology 7 days.

Thereafter, the PM-CPC was in dough-like state for a further 110-120 s before reaching the t_f at approximately 200 s. To investigate the potential impact of scaling up the manufacturing process, the batch size was increased from 1 g to 10 g. Analysis of the Gilmore needle test results demonstrated no statistically significant difference (p-value = 0.1) in either t_i or t_f for the optimal PM-CPC with the increased batch size, with both times remaining well within desired clinical specifications (Fig. 6a). The average values for t_i and t_f across the three batch sizes were 113.2 s and 190.5 s, respectively, thus aligning with the established clinical specifications.

Three hours after setting, the optimal PM-CPC exhibited an average compressive strength of 24.5 ± 4.6 MPa, with a failure strain of 2.5 ± 0.5 % across the different batch sizes (Fig. 6b). The bond strength of the optimal PM-CPC was not affected by the increase in powder batch size, demonstrating a bond strength of 3.9 ± 0.9 MPa (Fig. 6b). These values for both compressive strength and bond strength align with the clinical requirements.

3.3.2. Washout resistance

The optimal PM-CPC adhesive exhibited instant stability and integrity within 10 min, as evidenced by the absence of dissolution (Fig. 6c). Subsequent washout resistance testing demonstrated that the PM-CPC set before any visible disintegration occurred, thus passing the washout resistance test. These findings indicate that the adhesive demonstrates continuous stability under wet-field physiological conditions. The absence of disintegration in the adhesive suggests its ability to effectively bond to the bone surface. This characteristic is crucial for ensuring long-term durability and reliability in clinical applications.

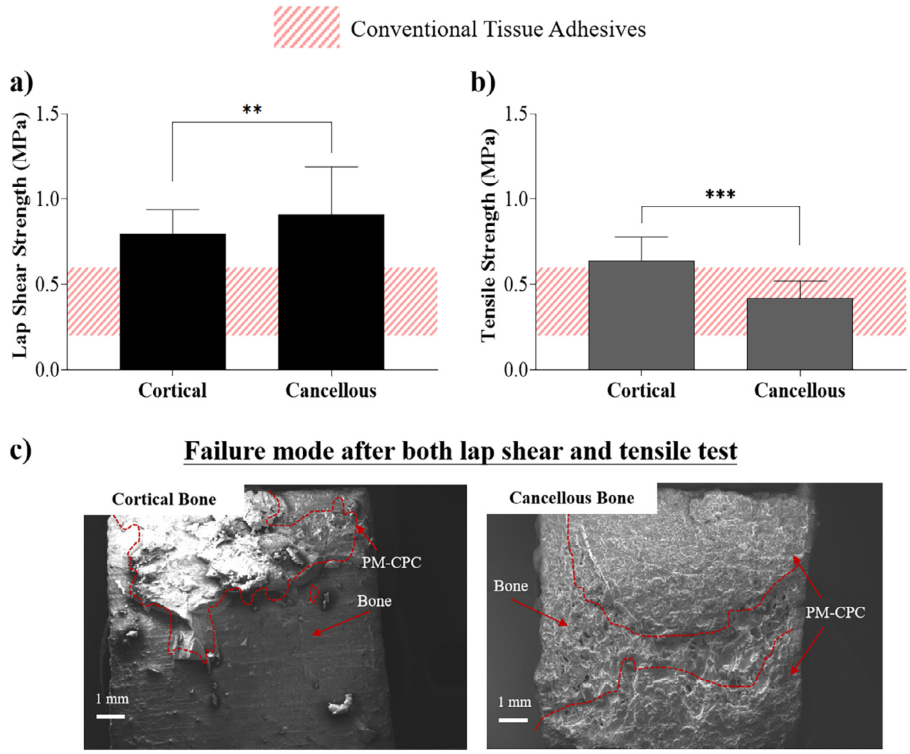

Fig. 7. a) Lap shear strength and b) tensile strength data shows the ability of optimal PM-CPC to adhere both cortical and cancellous bones, as well as the ability to withstand a force of approx. 100 N at 37ºC in a wet-field environment. c) SEM images illustrating the mixed-mode failure at the fracture surfaces of cortical and cancellous bone post-failure. $^{**}p$-value < 0.01 and $^{***}p$-value < 0.001.

3.3.3. Degradation properties

The degradation behaviour of the PM-CPC in PBS was evaluated over a 120-day study period, revealing an approximate total mass loss of 18 % (Fig. 6d). The degradation occurred gradually during the initial five days, resulting in approximately 5 % mass loss. Subsequently, the degradation rate decelerated, with an average daily mass loss of approximately 0.55 % observed between Day 5 and Day 30. From Day 30 onward, the mass loss stabilised, with no statistical difference between values recorded from Day 30 to Day 120.

Furthermore, the impact of introducing PPL enzyme into the PBS on degradation of the PM-CPC was investigated. The addition of PPL accelerated the degradation rate, leading to an approximate 25 % mass loss by Day 30 (Fig. 6d). During the initial five days of enzymatic degradation, the mass loss was 11.8 %. Subsequently, the rate of mass loss slowed, exhibiting a degradation pattern similar to that observed when tested in PBS alone in the absence of the enzyme.

3.3.4. Bioactivity

After 24 h of immersion in SBF, approximately 30 % of the α-TCP phase underwent transformation into HA crystals, and this proportion continued to increase over the subsequent four days (p-value $= 0.001$). XRD analysis showed that approximately 50 % of the calcium phosphate phase present has transformed into HA after seven days. SEM analysis depicted a newly formed layer on the surface of the PM-CPC after 24 h of SBF immersion, exhibiting chemical similarity to HA as confirmed by EDX analysis (Fig.6e). The SEM analysis further revealed the formation of needle-shaped crystals, with a length ranging from 7.70 µm to 27.04 µm and diameters between 1.5 µm and 3 µm. Samples immersed for 72 h exhibited an increased number of HA crystals, which were larger in size (both length and diameter), forming clusters on the surface without covering the entire sample. In contrast, the PM-CPC immersed for seven days demonstrated a complete apatite layer consisting of needle-shaped crystals with lengths between 70.18 µm and 145.06 µm and a diameter of 7.07 µm. Additionally, medium-sized (length: 8.3 µm, thickness: 3.4 µm) and large-sized (length: 82.3 µm, thickness: 19.9 µm) platelet crystals of HA were observed (Fig. 7e). The SEM EDX analysis confirmed the predominance of Ca and P elements on the surface. Evaluation of the Ca/P molar ratio of the apatite formed on the optimal PM-CPC recorded a value of 1.60, which closely resembles the typical Ca/P molar ratio of HA (1.62).

These findings demonstrate the successful conversion of the PM-CPC into HA through the immersion in SBF. The formation of a chemically similar HA layer on the surface of the PM-CPC and the presence of characteristic needle-shaped and platelet crystals validates its bioactive nature and potential for promoting osseointegration and bone regeneration.

3.4. Bone to bone adhesion properties – optimal PM-CPC

The bond strength of the optimal PM-CPC was evaluated using cancellous and cortical bone samples. Two different bond tests, namely, lap shear and tensile testing, were conducted in both wet and dry environments. Results showed that the optimal PM-CPC demonstrated higher bond strength values in a dry environment compared to wet conditions for both the cancellous and cortical bone samples. In dry environments, the lap shear strength values for cancellous bone samples were 9.3 ± 2.1 MPa, and the tensile strength values were 5.3 ± 1.3 MPa. In wet conditions, the corresponding values were significantly lower, with lap shear strength at 0.95 ± 0.28 MPa and tensile strength at 0.64 ± 0.14 MPa (Fig. 7a and b). Similar trends were observed for the cortical bone samples, where dry conditions resulted in lap shear and tensile strength values of 8.20 ± 0.3 MPa and 3.5 ± 1.5 MPa, respectively, while wet conditions yielded lower values of 0.80 ± 0.15 MPa and

0.5 ± 0.1 MPa respectively (Fig. 7a and b). Notably, despite the lower bond properties when tested in wet conditions, all femora bone samples exhibited higher resistance to loads compared to cortical bone samples, withstanding loads exceeding 50 N before fracture, with a maximum load of 100 N recorded. Furthermore, the bond strength values for cortical and cancellous bone samples surpassed those of conventional tissue adhesives, such as Histoacryl, Palcos LV and BSA-Glue, demonstrating significantly higher values (p-value = 0.04) [77,78] . The lap shear and tensile tests recorded strain values of approximately 5 % and 7–10 %, respectively, at the point of failure. It is worth mentioning that lap shear testing generated higher load values compared to the tensile test due to the increased exposure of osteons resulting from the cross-sectional cut, potentially enhancing micro-mechanical bonding, and consequently, enhancing bond strength.

To examine the failure mode of the optimal PM-CPC, SEM analysis was conducted on the fracture surfaces of cortical and cancellous bone samples. Mixed-mode failure, i.e., a combination of both cohesive and adhesive modes of failure, occurred in both lap shear and tensile testing of cancellous and cortical bone samples, as indicated by the representative SEM images. Lap shear and tensile samples for cortical bone obtained both cohesive and adhesive failure, with PM-CPC covering 51.03 mm^2, approximately 50 %, of the fracture surface area of. Similarly, cancellous bone, after either tensile or lap shear testing, was observed to fail by mixed-mode failure, with 82.6 % ± 5 % of the fracture surface showing cohesive-mode failure and 17.4 % ± 3 % of the fracture surface showing adhesive-mode failure.

4. Discussion

Bioadhesives offer potential for stabilising, repairing, and regenerating bone, as well as advantages over current fracture repair techniques. A critical clinical need exists for the development of adhesives that can replace the surgical need for metal hardware. Additionally, there is a growing demand for an adhesive that can be used in combination with traditional metal hardware to enhance fracture stability, minimise micromotion, and reduce the risk of loosening over time. To be suitable for fracture stabilisation and repair applications, a bone adhesive must provide early mechanical stability and exhibit optimal adhesive and cohesive properties in wet-field conditions. Although, calcium phosphate cements have been used effectively as bone void fillers, they suffer from limitations such as compromised biomechanical integrity, poor injectability, and slow setting times, which hamper their clinical effectiveness. In biological fluids, α-TCP, a bioactive and biodegradable calcium phosphate, undergoes transformation into HA within a relatively short period. A-TCP offers satisfactory biological properties and controlled biodegradation. In this study, phosphoserine, recreated complex architectural and material properties in α-TCP-based cements, resulting in significantly stronger adhesion to hard tissue and diverse biomaterial surfaces, enhanced handling, provision of a suitable template for mineralisation of nanoscale amorphous calcium phosphate, and stabilisation of metastable ceramic phases. DoE analysis highlighted the influence of the most significant factors (LPR, amount of phosphoserine and α-TCP powder particle size) on the final properties. Optimisation of the process yielded an injectable bone adhesive with setting, mechanical and adhesion properties suitable for clinical bone defect repair.

Initially, phase pure α-TCP was fabricated, with XRD analysis confirming the presence of α-TCP without any evidence of other calcium phosphates present, such as beta-TCP [79] and HA [80]. The presence of other phases could compromise the mechanical and biological properties of the resultant adhesive and therefore, achieving high phase purity is crucial to ensure biocompatibility and desired functionality, and to reduce the risk of implant failure or rejection [81–83]. The observed irregular, non-spherical, and polyhedral shape with a circularity of 0.35 ± 0.2 in the present study aligns with the reported morphology for α-TCP powders obtained through mechanical milling [84]. As expected, there was a negative correlation (R^2 = 0.90) between particle size and number of grinding cycles, consistent with previous findings [42]. The reduction in particle size can be attributed to the mechanical force exerted during the grinding process, which breaks down the larger particles into smaller ones. Additionally, the negative zeta potential obtained is advantageous for bone tissue engineering applications as it facilitates the adsorption of Ca^{2+} ions, promoting cell adhesion, proliferation and new bone formation [85,86].

A DoE study was then conducted to gain a comprehensive understanding of the factors influencing the handling and mechanical/adhesion properties of the adhesive. The DoE analysis demonstrated that the LPR, phosphoserine content, and the number of grinding cycles had the most significant impact on these properties, with the LPR showing the highest contribution. Increasing the LPR yielded an adhesive with enhanced injectability while concurrently reducing its setting and mechanical characteristics, in alignment with findings from previous investigations [42,47]. Conversely, increasing the phosphoserine content led to faster setting times, particularly for low levels of LPR, as phosphoserine acts as an accelerant in the setting reaction, thereby limiting the injection time window. Consequently, careful selection of LPR is necessary. The influence of the LPR on mechanical properties can be attributed to the effect the water content on the porosity of the adhesive after setting, where a higher water content results in increased porosity and poorer mechanical properties [87]. The DoE exhibited non-linear relationship between phosphoserine content and the mechanical properties. As the phosphoserine content is increased from 10 wt% to 25 wt%, there is a linear increase in compressive strength. This indicates a positive correlation between phosphoserine content and the mechanical properties of the CPC. However, beyond 25 wt% of phosphoserine within the PM-CPC composition, a linear reduction in compressive strength was observed. This finding is consistent with prior research on the influence of phosphoserine in α-TCP, which revealed a decline in mechanical properties at high phosphoserine concentrations [47]. This non-linear relationship between phosphoserine content and the mechanical properties of the CPC suggests the presence of an optimum or threshold concentration. At lower phosphoserine levels (10 wt% to 25 wt%), the incorporation of phosphoserine appears to enhance the interfacial bonding and chemical interactions within the matrix, leading to improved compressive strength. However, at higher phosphoserine levels (beyond 25 wt%), an excess of phosphoserine might disrupt the formation of the cement matrix or introduce structural irregularities, resulting in a decrease in compressive strength. Overall, the DoE models development here provided important insight into the relationships between multiple input and output variables in the context of the PM-CPC synthesis, enabling optimisation of the process.

Optimisation of the PM-CPC adhesive was then carried out using the DoE models to identify the optimal PM-CPC composition for clinical use, that demonstrates a satisfactory injectability and workability, and setting times within an appropriate range, along with enhanced mechanical and adhesion performance. The optimal composition for PM-CPC adhesive, meeting these clinical requirements, was determined to be 74 wt% α-TCP (after 11 grinding cycles), 25 wt% phosphoserine, 1 wt% calcium silicate, and an LPR of 0.3 mL/g. The optimal composition proposed by the DoE studies resulted in an injectable adhesive with setting times and static mechanical properties that met the required clinical specifications for the treatment of challenging bone fractures. Furthermore, exploring the influence of increasing the batch size showed that batch size had no effect on the setting and mechanical properties, indicating that it is feasible to scale up the fabrication process to produce industry relevant volumes.

Setting times for the optimal PM-CPC of 2.5–3.5 min were achieved. The fast setting indicates accelerated HA nucleation in the presence of phosphoserine, providing working and setting times within an acceptable range for surgeons to apply and stabilise bone fracture. While a rapid setting time post mixing is highly desirable from a clinical perspective, this poses challenges relating to the injectability of the adhesive. Prior investigations on cements for dental application have demonstrated the benefits associated with the minimally invasive administration of a biphasic calcium phosphate adhesive paste, facilitated through the using a dual-phase syringe system [25,56,88]. Therefore, it is envisaged that transitioning from the current manual mixing approach to a mechanised on-demand mixing technique will enable the precise and minimally invasive application of the PM-CPC cements developed herein. Our forthcoming efforts will concentrate on the development of a dual-phase syringe system tailored to meet the precise requirement for mixing and delivery of PM-CPC. The compressive (24.5 ± 4.6 MPa) and bond strength (3.9 ± 0.9 MPa) of the optimal PM-CPC also met the clinical requirements. Experimental validation confirmed the high accuracy and reliability of these models, which increased efficiency and flexibility by enabling simultaneous evaluation of multiple factors and quick identification of the critical factors and their optimal levels with fewer runs compared to traditional methods. Consequently, the optimal PM-CPC composition was identified using a rapid and cost-effective approach, while ensuring consistently reliable results. This was made possible by the statistical framework of DoE, which instilled higher confidence in the obtained outcomes. The incorporation of phosphoserine into the α-TCP cement enhanced its cohesion properties and accelerated the setting time, as evidenced by cohesive failure observed in the SEM analysis of the fracture surfaces. This cohesive failure indicates the formation of strong bonding between the PM-CPC and the substrate of the bone sample, a desirable property for clinical applications.

The optimal PM-CPC also demonstrated suitable degradation properties with ~25 % degradation observed by week 2. The degradation results were consistent with previous studies [89,90], showing slow degradation rates under physiological conditions. For instance, Ruhe et al. [91] fabricated calcium phosphate cements enhanced with poly (D,L-lactic-co-glycolic) acid (PLGA) that showed degradation of 30–40 % after 12 weeks, with only 10–20 % degradation during the initial 6 weeks. The PM-CPC provided effective support and stability for bone fragments during the initial stages of the natural bone healing process, as demonstrated by the slow initial degradation within the first five days. The overall slow rate of degradation aligns with the normal rate of bone healing and new bone formation [92]. Furthermore, the presence of an interfacial apatite layer on the PM-CPC surface, formed after immersion in SBF for seven days, confirms its bioactivity and suitability for biomedical applications. The formation of an interfacial apatite layer at the bone-biomaterials interface is a common characteristic of bioactive materials [93]. Overall, the slow degradation rate means that the PM-CPC can provide effective support and stability to bone fragments during the initial stages of the natural bone healing process.

In addition to the optimal handling and mechanical properties, the PM-CPC provided effective bone-to-bone bonding when used to adhere cancellous and cortical bovine femoral bone. The setting condition (dry or wet) significantly influenced the bond strength, with the optimal PM-CPC exhibiting a higher bond strength in dry environments compared to wet environments for both cancellous and cortical bone samples. This finding is consistent with previous studies reporting the adverse effects of moisture on the bonding properties of various biomaterials, including dental adhesives and bone cements [94]. Lower bond strength values under wet-field conditions can be attributed to the presence of moisture, which interferes with the PM-CPC-bone interface and induces hydrolytic degradation of the adhesive. Despite lower bond strength values under wet-field conditions, all femora bone samples withstood forces > 50 N before fracture, with a maximum load of 100 N recorded. This provides significantly higher bonding compared to other commercially available cements [77]. Cochran et al. demonstrated the immediate and sustained stabilisation of a dental implant within an oversized osteotomy in a canine mandibular model, achieved through the application of a calcium phosphate composition comprising 61.5% w/w, primarily composed of tetra-calcium phosphate (TTCP) phase, alongside 38.5% w/w phosphoserine) [59]. The histological examination of the implant site demonstrated a progressive replacement of the adhesive material by bone tissue, establishing and maintaining durable hard tissue for up to one year [58]. An extended-term investigation using this adhesive formulation further illustrated the gradual substitution of the biomaterial, thereby ensuring continuous osseointegration and the long-term maintenance of stability throughout a 12-month follow-up period [51]. The mixed-mode failure observed in the lap shear and tensile testing of cancellous and cortical bone samples indicates the presence of both molecular and physical bonds at the PM-CPC-bone interface. These results are consistent with other biomaterials (i.e., PMMA, Palacos BSA-glue etc.), whereby mixed-mode failure was described as the common mode of failure at the biomaterial-bone interface [77,78]. Mixed-mode failure leads to a more gradual and controlled failure mode, improving mechanical stability and reducing stress concentrations at the PM-CPC-substrate interface.

Taken together, these results demonstrate the successful development of an optimal PM-CPC adhesive with setting, mechanical, adhesion and degradation properties that potentially meets the clinical requirement for an injectable adhesive suitable for orthopaedic and dental applications.

5. Conclusions

In conclusion, the present study successfully demonstrated the potential of PM-CPC as a bioinspired adhesive for the stabilisation and repair of bone fractures. By applying a DoE approach, the composition of PM-CPC was optimised, with a particular focus on the LPR and phosphoserine content. The results obtained from the DoE analysis revealed that the LPR and phosphoserine content significantly influenced the handling, mechanical, and bond properties of the PM-CPC. Through the optimisation process, an optimal formulation has been identified, exhibiting compressive strength and bond/shear strength within the desired clinical ranges after a 24 h setting reaction. Moreover, the optimal PM-CPC composition required a short mixing time of 20 s and displayed an initial setting time of 3–4 min, allowing for homogenous mixing and precise delivery within a surgical setting. Notably, the PM-CPC demonstrated a high bone-to-bone adhesive bond strength under wet-field conditions, displaying its potential for effective bonding in challenging clinical scenarios in both orthopaedic and dental applications. Furthermore, the PM-CPC exhibited a slow degradation rate during the initial five days, providing crucial support and stability to bone fragments during the critical early stages of the natural bone healing process. The developed PM-CPC formulations met the clinical requirements for working and setting times, static mechanical properties, degradation properties, and injectability, making them highly suitable for surgical application to effectively stabilise and repair complex bone fractures.

In summary, the findings from this study highlight the remarkable potential of PM-CPC as an advanced biomaterial for bone fracture stabilisation and repair. The optimisation of its composition, coupled with its desirable mechanical and bonding properties, make it a promising candidate for clinical translation. Comprehensive further studies, encompassing both *in vitro* and *in vivo* studies, are imperative to thoroughly evaluate the efficacy, biocompatibility, and regenerative capabilities of the optimised PM-CPC composition derived through the detailed DoE optimisation process delineated in this research.

Declaration of Competing Interest

The authors declare no conflict of interest.

Funding

The research conducted in this study was funded by the Irish Research Council (Government of Ireland Scholarship Scheme) under award number GOIPG/2029/371 and the Irish Department of Enterprise, Trade and Employment (Disruptive Technologies Innovation Fund) under award number DT20200177.

Acknowledgments

The authors would like to acknowledge the research support provided by the Irish Research Council Government of Ireland Postgraduate Scholarship Award (GOIPG/2020/371) and the Irish Department of Enterprise, Trade and Employment Disruptive Technologies Innovation Fund Award (DT20200177). The particle size and zeta potential measurements were carried out at the Nano Research Facility in Dublin City University, which was funded under the Programme for Research in Third Level Institutions (PRTLI) Cycle 5. The PRTLI is cofunded through the European Regional Development Fund (ERDF), part of the European Union Structural Funds Programme 2011–2015; X-ray diffraction facilities of the Advanced Materials and Bioengineering Research (AMBER)/CRANN Institute in Trinity College Dublin were used for the chemical characterisation of the powders.

References

[1] S. Meena, P. Sharma, A.K. Sambharia, A. Dawar, Fractures of distal radius: an overview, J. Fam. Med. Prim. Care. 3 (2014) 325–332, doi:10.4103/2249-4863.148101.
[2] G. Zhu, T. Zhang, M. Chen, K. Yao, X. Huang, B. Zhang, Y. Li, J. Liu, Y. Wang, Z. Zhao, Bone physiological microenvironment and healing mechanism: basis for future bone-tissue engineering scaffolds, Bioact. Mater. 6 (2021) 4110–4140, doi:10.1016/j.bioactmat.2021.03.043.
[3] T.K. Kovach, A.S. Dighe, P.I. Lobo, Q. Cui, Interactions between MSCs and immune cells.pdf, J. Immunol. Res. 2015 (2015) 1–17.
[4] N. Sargioti, T.J. Levingstone, E.D. O'Cearbhaill, H.O. McCarthy, N.J. Dunne, Metallic microneedles for transdermal drug delivery: applications, fabrication techniques and the effect of geometrical characteristics, Bioengineering 10 (2022) 24, doi:10.3390/bioengineering10010024.
[5] D.S. Elliott, K.J.H. Newman, D.P. Forward, D.M. Hahn, B. Ollivere, K. Kojima, R. Handley, N.D. Rossiter, J.J. Wixted, R.M. Smith, C.G. Moran, A unified theory of bone healing and nonunion, Bone Jt. J. 98B (2016) 884–891, doi:10.1302/0301-620X.98B7.36061.
[6] D.B. Sneag, K.C. Zochowski, E.T. Tan, MR neurography of peripheral nerve injury in the presence of orthopedic hardware: technical considerations, Radiology 300 (2021) 246–259, doi:10.1148/radiol.2021204039.
[7] B.A. Peterkin, M.F. Reiter, M.R. Drzala, The significance of metal sensitivity testing in instrumented orthopaedic surgery, J. Ortho. Physician Assist. 8 (2020) 1–18, doi:10.2106/JBJS.JOPA.19.00039.
[8] A. Tzagiollari, H.O. McCarthy, T.J. Levingstone, N.J. Dunne, Biodegradable and biocompatible adhesives for the effective stabilisation, repair and regeneration of bone, Bioengineering 9 (2022) 250, doi:10.3390/bioengineering9060250.
[9] Y. Zaokari, A. Persaud, A. Ibrahim, Biomaterials for adhesion in orthopedic applications: a review, Eng. Regen. 1 (2020) 51–63, doi:10.1016/j.engreg.2020.07.002.
[10] N.F. Nuswantoro, M.A.R. Lubis, D. Juliadmi, E. Mardawati, P. Antov, L. Kristak, L.S. Hua, Bio-based adhesives for orthopedic applications: sources, preparation, characterization, challenges, and future perspectives, Designs 6 (2022) 1–24, doi:10.3390/designs6050096.
[11] J. Zhang, W. Liu, V. Schnitzler, F. Tancret, J.M. Bouler, Calcium phosphate cements for bone substitution: chemistry, handling and mechanical properties, Acta Biomater. 10 (2014) 1035–1049, doi:10.1016/j.actbio.2013.11.001.
[12] D.F. Farrar, Bone adhesives for trauma surgery: a review of challenges and developments, Int. J. Adhes. Adhes. 33 (2012) 89–97, doi:10.1016/j.ijadhadh.2011.11.009.
[13] H.H.K. Xu, J.B. Quinn, Calcium phosphate cement containing resorbable fibers for short-term reinforcement and macroporosity, Biomaterials 23 (2002) 193–202, doi:10.1016/S0142-9612(01)00095-3.
[14] K.L. Low, S.H. Tan, S.H.S. Zein, J.A. Roether, V. Mouriño, A.R. Boccaccini, Calcium phosphate-based composites as injectable bone substitute materials, J. Biomed. Mater. Res. - Part B Appl. Biomater. 94 (2010) 273–286, doi:10.1002/jbm.b.31619.
[15] B. Qiao, D. Zhou, Z. Dai, W. Zhao, Q. Yang, Y. Xu, X. Li, J. Wu, S. Guo, D. Jiang, Bone plate composed of a ternary nanohydroxyapatite/polyamide 66/glass fiber composite: biocompatibility in vivo and internal fixation for canine femur fractures, Adv. Funct. Mater. 29 (2019) 1–9, doi:10.1002/adfm.201808738.
[16] D. Barati, J.D. Walters, S.R. Pajoum Shariati, S. Moeinzadeh, E. Jabbari, Effect of organic acids on calcium phosphate nucleation and osteogenic differentiation of human mesenchymal stem cells on peptide functionalized nanofibers, Langmuir 31 (2015) 5130–5140, doi:10.1021/acs.langmuir.5b00615.
[17] J. Chung, I. Granja, M.G. Taylor, G. Mpourmpakis, J.R. Asplin, J.D. Rimer, Molecular modifiers reveal a mechanism of pathological crystal growth inhibition, Nature 536 (2016) 446–450, doi:10.1038/nature19062.
[18] L. Pastero, M. Bruno, D. Aquilano, Habit change of monoclinic hydroxyapatite crystals growing from aqueous solution in the presence of citrate ions: the role of 2D epitaxy, Crystals 8 (2018) 1–12, doi:10.3390/cryst8080308.
[19] M. Li, J. Zhang, L. Wang, B. Wang, C.V. Putnis, Mechanisms of modulation of calcium phosphate pathological mineralization by mobile and immobile small-molecule inhibitors, J. Phys. Chem. B 122 (2018) 1580–1587, doi:10.1021/acs.jpcb.7b10956.
[20] F. Buchanan, L. Gallagher, V. Jack, N. Dunne, Short-fibre reinforcement of calcium phosphate bone cement, Proc. Inst. Mech. Eng. Part H J. Eng. Med. 221 (2007) 203–211, doi:10.1243/09544119JEIM235.
[21] R.M. O'Hara, J.F. Orr, F.J. Buchanan, R.K. Wilcox, D.C. Barton, N.J. Dunne, Development of a bovine collagen-Apatitic calcium phosphate cement for potential fracture treatment through vertebroplasty, Acta Biomater. 8 (2012) 4043–4052, doi:10.1016/j.actbio.2012.07.003.
[22] J.L. Bystrom, M. Pujari-Palmer, Phosphoserine functionalized cements preserve metastable phases, and reprecipitate octacalcium phosphate, hydroxyapatite, dicalcium phosphate, and amorphous calcium phosphate, during degradation, in vitro, J. Funct. Biomater. 10 (2019) 1–20, doi:10.3390/jfb10040054.
[23] A. Kirillova, O. Nillissen, S. Liu, C. Kelly, K. Gall, Reinforcement and fatigue of a bioinspired mineral–organic bioresorbable bone adhesive, Adv. Healthc. Mater. 10 (2021) 1–19, doi:10.1002/adhm.202001058.
[24] R.T. Tran, L. Wang, C. Zhang, M. Huang, W. Tang, C. Zhang, Z. Zhang, D. Jin, B. Banik, J.L. Brown, Z. Xie, X. Bai, J. Yang, Synthesis and characterization of biomimetic citrate-based biodegradable composites, J. Biomed. Mater. Res. - Part A 102 (2014) 2521–2532, doi:10.1002/jbm.a.34928.
[25] R. O'Neill, H.O. McCarthy, E.B. Montufar, M.P. Ginebra, D.I. Wilson, A. Lennon, N. Dunne, Critical review: injectability of calcium phosphate pastes and cements, Acta Biomater. 50 (2017) 1–19, doi:10.1016/j.actbio.2016.11.019.
[26] N. Dunne, C. Mitchell, Biomedical/bioengineering Applications of Carbon Nanotube-Based Nanocomposites, Woodhead Publishing Limited, 2011, doi:10.1533/9780857091390.3.676.
[27] J. Luo, J. Faivre, H. Engqvist, C. Persson, The addition of poly(vinyl alcohol) fibers to apatitic calcium phosphate cement can improve its toughness, Materials (Basel) 12 (2019), doi:10.3390/ma12091531.
[28] R.A. Perez, H.W. Kim, M.P. Ginebra, Polymeric additives to enhance the functional properties of calcium phosphate cements, J. Tissue Eng. 3 (2012) 1–20, doi:10.1177/2041731412439555.
[29] J. Kozłowska, A. Sionkowska, Effects of different crosslinking methods on the properties of collagen-calcium phosphate composite materials, Int. J. Biol. Macromol. 74 (2015) 397–403, doi:10.1016/j.ijbiomac.2014.12.023.
[30] S. Shahbazi, F. Moztarzadeh, G.M.M. Sadeghi, Y. Jafari, In vitro study of a new biodegradable nanocomposite based on poly propylene fumarate as bone glue, Mater. Sci. Eng. C. 69 (2016) 1201–1209, doi:10.1016/j.msec.2016.08.035.
[31] M. Erken, A. Tevlek, P. Hosseinian, B. Topuz, H.M. Aydin, Effects of ceramic particle size on cell attachment and viability in polyurethane-based bone adhesive composites, J. Compos. Mater. 54 (2020) 2013–2022, doi:10.1177/0021998319884729.
[32] R.M. Khashaba, M.M. Moussa, D.J. Mettenburg, F.A. Rueggeberg, N.B. Chutkan, J.L. Borke, Polymeric-calcium phosphate cement composites-material properties: in vitro and in vivo investigations, Int. J. Biomater. 2010 (2010) 1–14, doi:10.1155/2010/691452.
[33] B. Huang, G. Caetano, C. Vyas, J.J. Blaker, C. Diver, P. Bártolo, Polymer-ceramic composite scaffolds: the effect of hydroxyapatite and β-tri-calcium phosphate, Materials (Basel) 11 (2018), doi:10.3390/ma11010129.
[34] Z. Wang, Z. Xu, W. Zhao, N. Sahai, A potential mechanism for amino acid-controlled crystal growth of hydroxyapatite, J. Mater. Chem. B 3 (2015) 9157–9167, doi:10.1039/c5tb01036e.
[35] F. Manoli, J. Kanakis, P. Malkaj, E. Dalas, The effect of aminoacids on the crystal growth of calcium carbonate, J. Cryst. Growth 236 (2002) 363–370, doi:10.1016/S0022-0248(01)02164-9.
[36] W. Jiang, M.S. Pacella, Di. Athanasiadou, V. Nelea, H. Vali, R.M. Hazen, J.J. Gray, M.D. McKee, Chiral acidic amino acids induce chiral hierarchical structure in calcium carbonate, Nat. Commun. 8 (2017) 1–13, doi:10.1038/ncomms15066.
[37] M. Bohner, H.P. Merkle, P. Van Landuyt, G. Trophardy, J. Lemaitre, Effect of several additives and their admixtures on the physico-chemical properties of

a calcium phosphate cement, J. Mater. Sci. Mater. Med. 11 (2000) 111–116, doi:10.1023/A:1008997118576.
[38] K. Rubini, E. Boanini, A. Bigi, Role of aspartic and polyaspartic acid on the synthesis and hydrolysis of brushite, J. Funct. Biomater. 10 (2019) 1–12, doi:10.3390/jfb10010011.
[39] S. Li, L. Wang, Phosphorylated osteopontin peptides inhibit crystallization by resisting the aggregation of calcium phosphate nanoparticles, CrystEngComm 14 (2012) 8037–8043, doi:10.1039/c2ce26140e.
[40] C.W. Prince, T. Oosawa, W.T. Butler, M. Tomana, A.S. Bhown, M. Bhown, R.E. Schrohenloher, Isolation, characterization, and biosynthesis of a phosphorylated glycoprotein from rat bone, J. Biol. Chem. 262 (1987) 2900–2907.
[41] A. Reinstorf, M. Ruhnow, M. Gelinsky, W. Pompe, U. Hempel, K.W. Wenzel, P. Simon, Phosphoserine - a convenient compound for modification of calcium phosphate bone cement collagen composites, J. Mater. Sci. Mater. Med. 15 (2004) 451–455, doi:10.1023/B:JMSM.0000021119.14870.3d.
[42] V. Jack, F.J. Buchanan, N.J. Dunne, Particle attrition of α-tricalcium phosphate: effect on mechanical, handling, and injectability properties of calcium phosphate cements, Proc. Inst. Mech. Eng. Part H - J. Eng. Med 222 (2008) 19–28, doi:10.1243/09544119JEIM312.
[43] C. Combes, C. Rey, Amorphous calcium phosphates: synthesis, properties and uses in biomaterials, Acta Biomater. 6 (2010) 3362–3378, doi:10.1016/j.actbio.2010.02.017.
[44] S. Von Euw, W. Ajili, T.H.C. Chan-Chang, A. Delices, G. Laurent, F. Babonneau, N. Nassif, T. Azaïs, Amorphous surface layer versus transient amorphous precursor phase in bone – a case study investigated by solid-state NMR spectroscopy, Acta Biomater. 59 (2017) 351–360, doi:10.1016/j.actbio.2017.06.040.
[45] A. Kirillova, C. Kelly, N. von Windheim, K. Gall, Bioinspired mineral-organic bioresorbable bone adhesive, Adv. Healthc. Mater. 7 (2018) e1800467, doi:10.1002/adhm.201800467.
[46] V. Bhagat, M.L. Becker, Degradable adhesives for surgery and tissue engineering, Biomacromolecules 18 (2017) 3009–3039, doi:10.1021/acs.biomac.7b00969.
[47] M. Pujari-Palmer, H. Guo, D. Wenner, H. Autefage, C.D. Spicer, M.M. Stevens, O. Omar, P. Thomsen, M. Edén, G. Insley, P. Procter, H. Engqvist, A novel class of injectable bioceramics that glue tissues and biomaterials, Materials (Basel) 11 (2018) 1–15, doi:10.3390/ma11122492.
[48] J.L. Bystrom, M. Pujari-Palmer, Phosphoserine functionalized cements preserve metastable phases, and reprecipitate octacalcium phosphate, hydroxyapatite, dicalcium phosphate, and amorphous calcium phosphate, during degradation, in vitro, J. Funct. Biomater. 10 (2019), doi:10.3390/jfb10040054.
[49] L. Offer, V. Bastian, T. Pavlidis, C. Heiss, M. Gelinsky, A. Reinstorf, S. Wenisch, K.S. Lips, R. Schnettler, Phosphoserine-modified calcium phosphate cements: bioresorption and substitution, Ann. Am. Thorac. Soc. 12 (2010) 181–204, doi:10.1002/term.
[50] R. Mai, R. Lux, P. Proff, G. Lauer, W. Pradel, H. Leonhardt, A. Reinstorf, M. Gelinsky, R. Jung, U. Eckelt, T. Gedrange, B. Stadlinger, O-phospho-L-serine: a modulator of bone healing in calcium-phosphate cements, Biomed. Tech. 53 (2008) 229–233, doi:10.1515/BMT.2008.040.
[51] D.L. Cochran, A.A. Jones, R. Sugita, M.C. Brown, H. Prasad, G.W. Kay, Twelve-month evaluation of a novel mineral-organic adhesive material used to stabilize dental implants placed in oversized osteotomies in vivo in an animal model, Clin. Oral Implants Res. 33 (2022) 391–404, doi:10.1111/clr.13899.
[52] M.R. Norton, G.W. Kay, M.C. Brown, D.L. Cochran, Bone glue - The final frontier for fracture repair and implantable device stabilization, Int. J. Adhes. Adhes. 102 (2020) 102647, doi:10.1016/j.ijadhadh.2020.102647.
[53] G. Hulsart-Billström, C. Stelzl, P. Procter, M. Pujari-Palmer, G. Insley, H. Engqvist, S. Larsson, In vivo safety assessment of a bio-inspired bone adhesive, J. Mater. Sci. Mater. Med. 31 (2020) 1–10, doi:10.1007/s10856-020-6362-3.
[54] F.P. Kesseli, C.S. Lauer, I. Baker, K.A. Mirica, D.W. Van Citters, Identification of a calcium phosphoserine coordination network in an adhesive organo-apatitic bone cement system, Acta Biomater. 105 (2020) 280–289, doi:10.1016/j.actbio.2020.01.007.
[55] K. Vrchovecká, M. Pávková-Goldbergová, H. Engqvist, M. Pujari-Palmer, Cytocompatibility and bioactive ion release profiles of phosphoserine bone adhesive: bridge from in vitro to in vivo, Biomedicines 10 (2022) 1–29, doi:10.3390/biomedicines10040736.
[56] L. Yang, S. Chen, T. Shang, R. Zhao, B. Yuan, X. Zhu, M.G. Raucci, X. Yang, X. Zhang, M. Santin, L. Ambrosio, Complexation of injectable biphasic calcium phosphate with phosphoserine-presenting dendrons with enhanced osteoregenerative properties, ACS Appl. Mater. Interfaces 12 (2020) 37873–37884, doi:10.1021/acsami.0c09004.
[57] A. Reinstorf, U. Hempel, F. Olgemöller, H. Domaschke, W. Schneiders, R. Mai, B. Stadlinger, A. Rösen-Wolff, S. Rammelt, M. Gelinsky, W. Pompe, O-phospho-L-serine modified calcium phosphate cements - material properties, in vitro and in vivo investigations, Materwiss. Werksttech. (2006), doi:10.1002/mawe.200600026.
[58] R. Sugita, A.A. Jones, G.A. Kotsakis, D.L. Cochran, Radiographic evaluation of a novel bone adhesive for maintenance of crestal bone around implants in canine oversized osteotomies, J. Periodontol. 93 (2022) 924–932, doi:10.1002/JPER.20-0876.
[59] D. Cochran, A. Jones, R. Sugita, M. Brown, T. Guda, H. Prasad, J. Ong, A. Pollack, G. Kay, Immediate dental implant stabilization in a canine model using a novel mineral-organic adhesive: 4-month results, Int. J. Oral Maxillofac. Implants 35 (2020) 39–51, doi:10.11607/jomi.7891.
[60] J. Singh, S.S. Chatha, H. Singh, Microstructural and in-vitro characteristics of functional calcium silicate topcoat on hydroxyapatite coating for bio-implant applications, Prog. Biomater. 11 (2022) 95–108, doi:10.1007/s40204-022-00183-w.
[61] Z. Du, H. Leng, L. Guo, Y. Huang, T. Zheng, Z. Zhao, X. Liu, X. Zhang, Q. Cai, X. Yang, Calcium silicate scaffolds promoting bone regeneration via the doping of Mg^{2+} or Mn^{2+} ion, Compos. Part B Eng. 190 (2020) 107937, doi:10.1016/j.compositesb.2020.107937.
[62] W. Liu, Z. Huan, C. Wu, Z. Zhou, J. Chang, High-strength calcium silicate-incorporated magnesium phosphate bone cement with osteogenic potential for orthopedic application, Compos. Part B Eng. 247 (2022) 110324, doi:10.1016/j.compositesb.2022.110324.
[63] G.C. Wang, Z.F. Lu, H. Zreiqat, 8-Bioceramics for skeletal bone regeneration, Bone Substit. Biomater. 1 (2014) 180–216, doi:10.1533/9780857099037.2.180.
[64] M. Cerrutti, N. Sahai, Silicate biomaterials for orthopaedic and dental implants, Rev. Miner. Geochem. 64 (2014) 283–313, doi:10.2138/rmg.2006.64.9.
[65] P. Zhou, D. Xia, Z. Ni, T. Ou, Y. Wang, H. Zhang, L. Mao, K. Lin, S. Xu, J. Liu, Calcium silicate bioactive ceramics induce osteogenesis through oncostatin M, Bioact. Mater. 6 (2021) 810–822, doi:10.1016/j.bioactmat.2020.09.018.
[66] C.C. Chen, C.C. Ho, C.H. David Chen, S.J. Ding, Physicochemical properties of calcium silicate cements for endodontic treatment, J. Endod. 35 (2009) 1288–1291, doi:10.1016/j.joen.2009.05.036.
[67] M.J. Anderson, P.J. Whitcomb, RSM simplified : optimizing processes using response surface methods for design of experiments, (n.d.).
[68] J. Jansen, E. Ooms, N. Verdonschot, J. Wolke, Injectable calcium phosphate cement for bone repair and implant fixation, Orthop. Clin. N. Am. (2005), doi:10.1016/j.ocl.2004.06.014.
[69] K.O. Böker, K. Richter, K. Jäckle, S. Taheri, I. Grunwald, K. Borcherding, J. von Byern, A. Hartwig, B. Wildemann, A.F. Schilling, W. Lehmann, Current state of bone adhesives-necessities and hurdles, Materials (Basel) 12 (2019) 1–19, doi:10.3390/ma12233975.
[70] N.A. Caraan, R. Windhager, J. Webb, N. Zentgraf, K.D. Kuehn, Role of fast-setting cements in arthroplasty: a comparative analysis of characteristics, World J. Orthop. 8 (2017) 881–890, doi:10.5312/wjo.v8.i12.881.
[71] R. Famery, N. Richard, P. Boch, Preparation of α- and β-tricalcium phosphate ceramics, with and without magnesium addition, Ceram. Int. 20 (1994) 327–336, doi:10.1016/0272-8842(94)90050-7.
[72] ISO 13320:2009 particle size analysis—laser diffraction methods, Part 1 Gen. Princ. (2009).
[73] H. Cement, M. Cabinets, M. Rooms, B. Statements, D. Mass, Standard test method for time of setting of hydraulic-cement paste by Gillmore, Water (Basel) (2010) 1–4.
[74] I. standard, Implants for surgery - acrylic resin cements, Iso 5833 (2002) 1–22.
[75] L.E. Carey, H.H.K. Xu, C.G. Simon, S. Takagi, L.C. Chow, Premixed rapid-setting calcium phosphate composites for bone repair, Biomaterials 26 (2005) 5002–5014, doi:10.1016/j.biomaterials.2005.01.015.
[76] T. Kokubo, H. Takadama, How useful is SBF in predicting in vivo bone bioactivity? Biomaterials 27 (2006) 2907–2915, doi:10.1016/j.biomaterials.2006.01.017.
[77] V. Lührs, S. Stößlein, K. Thiel, I. Grunwald, A. Hartwig, An in vitro bone-to-bone adhesion test method using the compression shear test, Int. J. Adhes. Adhes. 111 (2021) 102977, doi:10.1016/j.ijadhadh.2021.102977.
[78] A. Bou-Francis, A. Ghanem, Standardized methodology for in vitro assessment of bone-to-bone adhesion strength, Int. J. Adhes. Adhes. 77 (2017) 96–101, doi:10.1016/j.ijadhadh.2017.03.014.
[79] H.S. Ryu, H.J. Youn, K.S. Hong, B.S. Chang, C.K. Lee, S.S. Chung, An improvement in sintering property of β-tricalcium phosphate by addition of calcium pyrophosphate, Biomaterials 23 (2002) 909–914, doi:10.1016/S0142-9612(01)00201-0.
[80] H. Eslami, M. Solati-Hashjin, M. Tahriri, The comparison of powder characteristics and physicochemical, mechanical and biological properties between nanostructure ceramics of hydroxyapatite and fluoridated hydroxyapatite, Mater. Sci. Eng. C 29 (2009) 1387–1398, doi:10.1016/j.msec.2008.10.033.
[81] G. Cicek, E.A. Aksoy, C. Durucan, N. Hasirci, Alpha-tricalcium phosphate (α-TCP): solid state synthesis from different calcium precursors and the hydraulic reactivity, J. Mater. Sci. Mater. Med. 22 (2011) 809–817, doi:10.1007/s10856-011-4283-x.
[82] M.R. Cohn, A. Unnanuntana, T.J. Pannu, S.J. Warner, J.M. Lane, Materials in fracture fixation, Compr. Biomater. II 7 (2017) 278–297, doi:10.1016/B978-0-12-803581-8.10109-2.
[83] Y. Pan, F. Xiao, Y. Dong, Optimization of the preparation process of α-tricalcium phosphate applied to bone cement, Mater. Res. Express. 6 (2019), doi:10.1088/2053-1591/ab36fd.
[84] A. Bignon, J. Chevalier, G. Fantozzi, Effect of ball milling on the processing of bone substitutes with calcium phosphate powders, J. Biomed. Mater. Res. 63 (2002) 619–626, doi:10.1002/jbm.10379.
[85] A. Fahami, G.W. Beall, Mechanosynthesis of carbonate doped chlorapatite–ZnO nanocomposite with negative zeta potential, Ceram. Int. 41 (2015) 12323–12330, doi:10.1016/j.ceramint.2015.06.061.
[86] K. Cheng, W. Weng, H. Wang, S. Zhang, In vitro behavior of osteoblast-like cells on fluoridated hydroxyapatite coatings, Biomaterials 26 (2005) 6288–6295, doi:10.1016/j.biomaterials.2005.03.041.
[87] R. Martínez-García, M.I. Sánchez de Rojas, P. Jagadesh, F. López-Gayarre, J.M. Morán-del-Pozo, A. Juan-Valdes, Effect of pores on the mechanical and durability properties on high strength recycled fine aggregate mortar, Case Stud. Constr. Mater. 16 (2022) e01050, doi:10.1016/j.cscm.2022.e01050.
[88] U. Tariq, R. Hussain, K. Tufail, Z. Haider, R. Tariq, J. Ali, Injectable dicalcium phosphate bone cement prepared from biphasic calcium phosphate extracted

from lamb bone, Mater. Sci. Eng. C 103 (2019) 109863, doi:10.1016/j.msec.2019.109863.
[89] R.P. Félix Lanao, S.C.G. Leeuwenburgh, J.G.C. Wolke, J.A. Jansen, Bone response to fast-degrading, injectable calcium phosphate cements containing PLGA microparticles, Biomaterials 32 (2011) 8839–8847, doi:10.1016/j.biomaterials.2011.08.005.
[90] T. Lu, F. He, J. Ye, Physicochemical properties, in vitro degradation, and biocompatibility of calcium phosphate cement incorporating poly(lactic- co-glycolic acid) particles with different morphologies: a comparative study, ACS Omega 6 (2021) 8322–8331, doi:10.1021/acsomega.1c00031.
[91] P.Q. Ruhé, E.L. Hedberg-Dirk, N.T. Padron, P.H.M. Spauwen, J.A. Jansen, A.G. Mikos, Porous poly(DL-lactic-co-glycolic acid)/calcium phosphate cement composite for reconstruction of bone defects, Tissue Eng. 12 (2006) 789–800, doi:10.1089/ten.2006.12.789.
[92] C.S. Bahney, R.L. Zondervan, P. Allison, A. Theologis, J.W. Ashley, J. Ahn, T. Miclau, R.S. Marcucio, K.D. Hankenson, Cellular biology of fracture healing, J. Orthop. Res. 37 (2019) 35–50, doi:10.1002/jor.24170.
[93] S. Baradaran, E. Moghaddam, B. Nasiri-Tabrizi, W.J. Basirun, M. Mehrali, M. Sookhakian, M. Hamdi, Y. Alias, Characterization of nickel-doped biphasic calcium phosphate/graphene nanoplatelet composites for biomedical application, Mater. Sci. Eng. C 49 (2015) 656–668, doi:10.1016/j.msec.2015.01.050.
[94] A. Aminoroaya, R.E. Neisiany, S.N. Khorasani, P. Panahi, O. Das, H. Madry, M. Cucchiarini, S. Ramakrishna, A review of dental composites: challenges, chemistry aspects, filler influences, and future insights, Compos. Part B Eng. 216 (2021) 108852, doi:10.1016/j.compositesb.2021.108852.